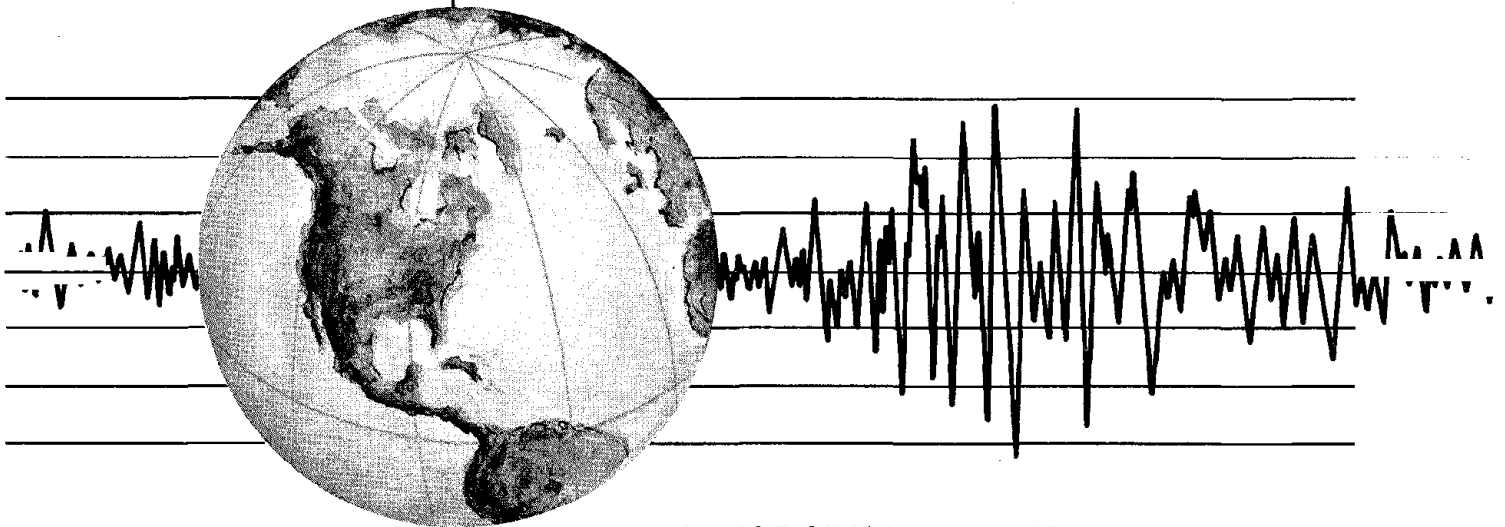EARTHQUAKE ENGINEERING RESEARCH CENTER

JOINT OPENING NONLINEAR MECHANISM:

INTERFACE SMEARED CRACK MODEL

by

JAMES SHAW-HAN KUO

COLLEGE OF ENGINEERING

UNIVERSITY OF CALIFORNIA · Berkeley, California

REPORT DOCUMENTATION PAGE	1. REPORT NO. NSF/CEE-82015	2.	3. Recipient's Accession No. PB83 149195

4. Title and Subtitle	5. Report Date
Joint Opening Nonlinear Mechanism: Interface Smeared Crack Model	August 1982
	6.

7. Author(s)	8. Performing Organization Rept. No.
James Shaw-Han Kuo	UCB/EERC-82/10

9. Performing Organization Name and Address	10. Project/Task/Work Unit No.
Earthquake Engineering Research Center University of California, Berkeley 47th Street and Hoffman Blvd. Richmond, Calif. 94804	
	11. Contract(C) or Grant(G) No.
	(C)
	(G) PFR-78-19333

12. Sponsoring Organization Name and Address	13. Type of Report & Period Covered
National Science Foundation 1800 G Street, N.W. Washington, D.C. 20550	
	14.

15. Supplementary Notes

16. Abstract (Limit: 200 words)

   In this report contraction joint opening behavior is studied. An economical model called the Interface Smeared Crack Model is developed to simulate the joint opening nonlinear mechanism. The model is based on the general smeared crack approach, with a specially introduced "pushing back" operation which is intended to correct the local structure response at element level. This method dramatically reduces the computational cost compared with that of a standard joint element analysis. It is demonstrated that it would be beneficial to include joint opening mechanism in the dynamic analysis of arch dams, because joint opening will limit the peak tensile arch stresses and thus improve the seismic resistance of the structure.

17. Document Analysis   a. Descriptors

b. Identifiers/Open-Ended Terms

c. COSATI Field/Group

18. Availability Statement	19. Security Class (This Report) UNCLASSIFIED	21. No. of Pages 91
Release Unlimited	20. Security Class (This Page) UNCLASSIFIED	22. Price

(See ANSI-Z39.18)   See Instructions on Reverse

OPTIONAL FORM 272 (4 (Formerly NTIS-35) Department of Commerce

JOINT OPENING NONLINEAR MECHANISM:
INTERFACE SMEARED CRACK MODEL

by

James Shaw-Han Kuo

Report to the National Science Foundation

August 1982

ABSTRACT

This report consists of Part II of the dissertation submitted by the author to the Graduate Division, University of California, Berkeley, in partial satisfaction of the requirements for the degree of Doctor of Philosophy in Engineering.

In this report the contraction joint opening behavior is studied. An economical model called the Interface Smeared Crack Model is developed to simulate the joint opening nonlinear mechanism. The model is based on the general smeared crack approach, with a specially introduced "pushing back" operation which is intended to correct the local structure response at element level. This method dramatically reduces the computational cost as compared with a standard joint element analysis. It is demonstrated that it would be beneficial to include the joint opening mechanism in the dynamic analysis of arch dams, because the joint opening will limit the peak tensile arch stresses and thus improve the seismic resistance of the structure.

ACKNOWLEDGEMENTS

Many people have assisted me during the course of my graduate studies. I am most thankful to Professor Ray W. Clough, my thesis advisor and the Chairman of my dissertation committee. His inspiration, patience and guidance are deeply appreciated, and I will always remember his fine example.

I am also grateful to Professors E. L. Wilson and C. D. Mote, members of my dissertation committee, for their valuable suggestions, encouragement and friendly guidance.

I wish to express my gratitude to Dr. John F. Hall for many valuable discussions during the first part of my research, and to Professor R. L. Taylor for making his computer program FEAP available.

This research has been part of the U.S.-R.O.C. Cooperative Research Program. Financial support from the Natioal Science Foundation is gratefully acknowledged. Computer facilities were provided by the Lawrence Berkeley Laboratory, University of California, Berkeley. I also want to thank Toni Avery for her excellent typing.

I am greatly indebted to Drs. Bill & Lydia Yap and Don & Nancy Mangold, two Christian couples, who provided care, concern and encouragement throughout my graduate studies.

Above all, I wish to express my gratitude to my family for their unfailing support, understanding, encouragement and love.

TABLE OF CONTENTS

LIST OF FIGURES

1. INTRODUCTION

1.1 Objectives

A concrete arch dam is constructed as a system of monolith blocks separated by vertical contraction joints. The monoliths are constructed separately so that cooling and shrinkage may take place independently in each. Therefore, the contraction joints between monoliths may be left open during the construction period, but after cooling and shrinkage have been stabilized, they are grouted under high pressure so that the dam may form a complete monolithic structure. When the reservoir is filled, the compressive **arch stresses** across the contraction joints are further increased, so the dam body behaves as a truly monolithic system with regard to static loads.

However, when the dam is subjected to intense earthquake ground motions, dynamic stresses are induced which oscillate between tension and compression as the structure vibrates. These dynamic stresses represent changes from the static stress state, and if a tensile dynamic component exceeds its corresponding compressive static component, a net tensile stress state is indicated.

Because of the way an arch dam is constructed, it is evident that net tensile arch stresses cannot exist across the contraction joints; instead, the joints will open as the dynamic tensile arch stresses exceed static compressive arch stresses, and thus reduce the arch stresses to zero across the joints (8). The net tensile arch stresses will then be redistributed to the rest of the dam body.

This joint-opening nonlinear structural behavior of an arch dam is the predominant nonlinear phenomenon associated with the response of an arch dam. It can be considered beneficial because it releases tensile arch

stresses locally and reduces the possibility of developing cracks in the concrete. Therefore, it is important to include the joint-opening non-linear mechanism in a general arch dam response analysis. As the joint-opening will reduce the peak tensile arch stresses and elongate the period of vibration, it is expected that it will improve the seismic resistance of arch dams, or, reduce the cost of construction.

It is the objective of this study to develop an economical mathematical model to simulate the joint-opening nonlinear mechanism in arch dams. The mathematical model, or the Interface Smeared Crack Model (ISCM), developed herein has the following features:

(1) No increase in the number of equations, as compared to the linear response analysis of arch dams;

(2) good representation of global structural response;

(3) reasonable representation of local structural behavior;

(4) possibility of extending to evaluate cantilever-cracking phenomena, the other major nonlinear mechanisms associated with the seismic response of arch dams (30).

1.2 State of the Art

Nonlinear arch dam response analyses including joint-opening nonlinear mechanisms are few in the literature (40-43). Priscu, et al. (40) used a quadratic programming approach for minimization of potential energy to deal with "pulvino" perimetral joints in an arch dam, so that no tensile stress will exist in the direction normal to the joint. Holand, et al. (41) and others investigated the formation of cracks in the dam, but no mathematical model was proposed to simulate their behavior.

Croucamp, et al.(42) used a double-noding finite element formulation to simulate the behavior of an opened joint, and studied stress patterns generated, in an arch dam and a multiple dome dam. Richetts, et al. (43)

employed special joint elements, that have been used successfully to simulate the behavior of interfaces of jointed rocks, for modelling the preformed cracks or weak planes. They have shown the difference in stresses, strains and displacements when the preformed cracks are included compared to results without precracked sections.

Although only limited works have been carried out with regard to the simulation of joint-opening behavior in arch dams, we could, as observed by Ricketts, find a vast literature that deals with analytical modelling of the behavior of joints, seams, cracks and interfaces. For example, in the literature of reinforced concrete structures (1-4,6,11,22-24,27, 32,33), we can find analytical models for simulating predefined cracks; in the literature of geomechanics (5,7,9,31), we can find special finite elements proposed for simulating interface joints between rock masses; in the literature of contact-impact problems (13-16,18-21), we can find mathematical models for dealing with the behavior of interfaces.

Because of their particular applications in their particular areas of interest, we will not go into discussion of how their models are useful in their own problems. However, later in Chapter 2, we will discuss in some depth how each model behaves and the relative advantages and disadvantages of various kinds of models. Also we will then select the most suitable, simplest and most economical model for our purpose.

1.3   Scope and Organization

Chapter 2 describes the joint-opening nonlinear structural behavior, it also discusses the essential features that are required of an analytical model for simulating the joint-opening behavior, and outlines the characteristics of the proposed model after reviewing several kinds of models proposed in the literature for simulating cracks or interfaces.

Chapter 3 presents the proposed model ISCM with all aspects of its computation and logic. The assumptions and limitations of the model, description of the concepts on which the model is derived, and the detailed modelling process are illustrated in depth.

In Chapter 4, computer implementation of ISCM with a proposed economical step-by-step integration scheme is presented, and several numerical examples to illustrate the proposed model are shown.

The studies contained in this volume are limited to the 2-D case only, but some further developments and factors involved in the extension to 3-D cases are mentioned in Chapter 5. Final concluding remarks are presented in Chapter 6.

2. DESCRIPTION OF THE JOINT-OPENING NONLINEAR MECHANISM

2.1 Behavior of the Joint-Opening Nonlinear Mechanism (Fig. II-1(a))

The contraction joints between monoliths of an arch dam can be considered as precracked interface sections; they could be constructed with or without shear keys. If they include shear keys providing high shear rigidity across the interfaces, they can guarantee the full shear transfer capacity across the joints. If shear keys are not provided, the shear transfer across the contraction joints could be evaluated either according to the Coulomb friction law or neglected completely.

As mentioned earlier, because of the construction process the contraction joints cannot resist any net tensile arch stresses, although these could be developed within the concrete monoliths. The net tensile arch stresses across the joints tend to open the joints and thus cause stress redistributions. In general, the redistribution may increase compressive stresses at some parts of the structure, reduce compressive stresses in other parts and enhance tensile stresses at yet other parts, all depending on the material properties, stress distributions and constraints of the structure. When the dam is subjected to dynamic loadings such as earthquake ground motions, due to stress reversals, the joints may oscillate between opened and closed states, while the net arch stresses across the joints oscillate between tension and compression.

The opening and closing of a joint is normally a gradual process, but when the closing moment at an opened joint is much larger than the axial force, then the moment will tend to produce an impact shock wave as it closes the joint suddenly. When the joint is closed with excessive compressive stresses, local compression damages may occur and cause effective softening of the material in the vicinity of the joint. This kind of

reduction in compressive strength of the material is considered to be a permanent effect.

Some monolith joints might be completely opened at an instant when tensile arch stresses are indicated throughout the joint. This kind of momentary loss of arch action may not necessarily fail the structure, because the monoliths still rest on stable supports. Therefore, if we only focus our attention on the joint-opening nonlinear mechanism, and are not concerned about possible cantilever failure due to horizontal cracking, the failure of the structure will occur only from compression failure of the concrete.

The softening of the structural system due to joint-openings will elongate the period of vibration of the structure, and thus may significantly change the amplification factor of the structural response. Therefore, it is important to include the effect of joint-opening in the dynamic response analysis of arch dams.

2.2 Considerations Concerning an Analytical Model for the Joints

We will now consider developing an analytical model according to the behavior of the joint-opening nonlinear mechanism described above.

For simplicity, our current investigation will be limited to joints with shear keys, that is, to joints with full shear transfer capacity; thus, no relative transverse displacement will occur at any contraction joint. Furthermore, for these preliminary studies an individual arch rib representing a horizontal section of an arch dam will be examined; the interface joints between blocks of the arch rib (Fig. II-1(b)) thus correspond to the contraction joints between monoliths of the arch dam.

To analytically model the behavior of precracked interface joints, the following factors must be considered:

(1) locations of the joints: the locations of the joints within the arch rib have to be identified through input to the computer program, either by introducing fictitious finite elements, or by indexing the joint with the element numbers of the blocks that it joins;

(2) joint-opening identification: criteria of joint-opening have to be set up for the model. Tensile normal stress across the joint will be an indication that the joint has opened or reopened (6,23,27).

(3) Joint-closure identification: criteria of closure of the joint also have to be established. Due to Poisson ratio effects, compressive normal stress across the joint may not bring the two sides of the joint into contact, therefore, compressive normal strain is chosen to indicate the closing or reclosing of the joint (6,23,27).

(4) Compressive strength: various constitutive models (1-4,17,23,24,27, 32,33) for concrete can be used and ultimate compressive strength could thus be specified accordingly. The simplest nonlinear constitutive relation, elastic-perfectly-plastic, will be used here.

(5) Computation of opening width: the width of joint-opening is an interesting quantitative value in the joint-opening phenomenon; its computation will depend on the analytical modelling process selected (1-7,9-16,18-27).

(6) Computation of opening ratio: the opening ratio is also a quantity of interest in the joint-opening phenomen; it is expressed as a percentage of opening into the joint. The computation of this ratio also depends on the analytical modelling process chosen; generally interpolation is used to locate the point of zero-opening along the joint. The opening ratio has a value of $\pm$ 1 when the joint is fully opened and separated, it has a value of zero when the joint is fully closed. Negative values indicate that the opening of the joint

is on the downstream face (30).

(7) Modification of material after joint-opening: material modification to account for the softening of the system after the joint has opened can be done in various ways, either by directly modifying the joint properties if it is included explicitly, or by modifying the adjacent concrete properties. Because of the great influence of material modification on the subsequent behavior of the structure, any modification of material properties after joint-opening should be justified rationally (1-7,9-16,18-27,32,33,36).

Bearing in mind the desired features of the analytical model as mentioned in Section 1.1, with these considerations we can now proceed to evaluate the analytical models available in the vast literature produced to date, and to search for or develop the model that is most economical and appropriate for our purpose.

2.3 Selecting Analytical Model for the Joints

A vast literature in gemechanics, reinforced concrete structures and contact-impact problems deals with analytical simulation of the behavior of joints, seams, cracks and interfaces. In general, the procedures can be classified into 3 categories: discrete crack models, smeared crack models, and special treatment. Due to its costly computational effect, little attention has been paid to discrete crack models, while special treatments generally are cumbersome. The smeared crack model has drawn the most attention because of its simplicity and economy, although it is only good for representation of global behavior. All these models are available for both static and dynamic nonlinear response analysis. Each has its own special features and their characteristics are described briefly in the following sections.

2.3.1 Discrete Crack Models

Discrete crack models in general include two kinds of elements: node-on-node spring or contact elements (Fig. II-2(a)) and joint elements (Fig. II-2(b)). Because of the additional degrees of freedom introduced, they normally require a large number of equations as compared with continuous linear systems, thus they are very expansive.

2.3.1.1 Node-on-Node Spring or Contact Elements (13-16,18-22)

Node-on-node spring or contact elements can be implemented most directly. When the spring force or contact force is in compression, its two end nodes are in contact and the spring constant assumes its full value. When the spring force or contact force indicates tension, the joint is opened, the two sides separate immediately, and the spring constant reduces to zero. Two techniques can be employed to set up the mathematical model. If the double-noding technique is used, the size of the system matrices does not change, the joint-opening is confined to predefined sections and the number of equations of the system always will be large. If the splitting-node technique is used, the dimension of the system matrices will vary and will require redefinition of the structural topology as the joints open and close. The opening width can be a direct output quantity and the opening ratio can be computed easily.

2.3.1.2 Joint Elements (5,7,9,11,31)

Joint elements require introducing additional relative degrees of freedom in the direction normal to the joint, with appropriate interpolation functions associated with these additional degrees of freedom, acting in the direction parallel to the joint. This model has the same number of equations as the double-noding technique mentioned above, and joint-

openings are also confined to predefined sections. Joint-opening is indicated by a positive relative normal displacement. Opening width is the amount of relative normal displacement and can be a direct output value; opening ratio can be computed easily by interpolation. But material modification of the joint element will be difficult when the joint is only opened half-way, unless we forfeit the entire joint element whenever part of it is opened. This will make it difficult to model gradual opening behavior of the joint using only one joint-element throughout a predefined interface joint. However, this model has favorable attributes in that it can localize structural nonlinearities of various kinds into such an element; also it can be easily implemented in a general finite element analysis code because it is formulated like a standard finite element.

As a summary concerning the simulation of the interface joint behavior, the discrete crack model has these advantages:

(1) It is in agreement with the actual physical phenomenon: it realistically produces a crack, a strain discontinuity, by separating the joint into two sides;

(2) it provides good representation of local behavior, such as stress or strain variations; the opening width can be a direct output quantity without any ambiguity, and opening ratio can be easily calculated.

and disadvantages:

(1) It requires a large number of equations in the system, thus is very costly in computation;

(2) in some cases, it requires redefinition of the structural topology successively as the joints are opened and closed;

(3) partial material modification is difficult when the joint-opening is only partial because the joints open gradually.

2.3.2 Smeared Crack Models (6,10,23,27,33)

The smeared crack model has been the most popular modelling process since it first appeared. It can model the global structural behavior fairly accurately but not the local behavior. Its basic principle is to smear out the local cracks associated with a integration point into the tributary region of this integration point (Fig. II-2(c)). The effective result is redistribution of the strain energy which computationally is lumped at integration points. Since the finite element solution is obtained by minimizing the total potential energy of the structural system, if the strain energy released by smeared out cracks is equivalent to that of the local cracks, the global structural behavior is expected to be accurate. Similar global results have been obtained for different kinds of material property modifications associated with smeared out cracks, thus it is evident that the global structural behavior is insensitive to the local material modifications as long as the modifications can release an equivalent amount of strain energy due to the cracks. Because of this lack of sensitivity, the smeared crack model is not able to model local structural behavior well, unless some special local operations are introduced according to the actual physical behavior.

As a summary concerning the simulation of the interface joint behavior, the smeared crack model has these advantages:

(1) It has the same number of equations as the continuous system;

(2) cracks are smeared out, therefore no redefinition of structural topology is needed;

(3) it includes cracks by local material modifications which can easily account for partial joint-opening, and there is no need to recalculate values of element interpolation functions or their derivatives;

(4) it can model global structural behavior fairly accurately;

(5) the cracks or interface joints can be included anywhere in the structure easily.

and disadvantages:

(1) it is not in agreement with the actual physical phenomenon; no strain discontinuity is represented across cracks, the structural topology includes no discontinuities;

(2) it is not able to describe well the local structural behavior such as stress or strain variations, opening width and opening ratio values. Only the stress normal to the crack is correctly represented;

(3) the arbitrary local material modifications may lead to misrepresentation of the failure mechanism of the structure. If cracks have been integrated over a major part of the structural system, the global structural behavior will be erroneous when local material modifications are not properly performed.

2.3.3 Special Treatments (1-4,10,25)

Some models for cracks involve specially introduced crack properties. An equilibrium model has been proposed with natural boundary displacements and an initial strain concept (25). Also there is crack model with relative strain representing relative displacement across a crack (10). Yet another crack model introduces special local degrees of freedom with a special integration scheme to account for crack opening properties (1-4). All of these have their own particular attributes although all are restricted in some way, and their capabilities for treating cracks or interface joints are noteworthy. We will not go into details here, but interested readers should consult the references.

2.3.4 <u>Characteristics of the Proposed Model</u>

Considering the desired features of an analytical model mentioned in Section 1.1 and all the models available in the literature, we propose a simple and economical model, based on the smeared crack concept with a local "pushing-back" operation introduced at the element level which, with minimal expense, can compensate for some of the defects of smeared crack models. The pushing-back operation is empirical and is established on the criterion that each block between two consecutive joints must be at its best equilibrium position. The model we will present is limited to small displacement structural behavior, the joint-opening is initiated by tensile normal stress across the joint and closure is indicated by compressive normal strain. Material nonlinearity is lumped at joints and its constitutive relation is defined according to an "equivalent uniaxial strain" material model (32,33). Local material modifications which will produce localized anisotropy are carried out so as to retain symmetry of the stiffness matrices. Opening width is computed empirically and the opening ratio is found by interpolation on equivalent normal displacements rather than on normal strains.

The proposed model, namely, the Interface Smeared Crack Model, is detailed in the following chapter.

3. INTERFACE SMEARED CRACK MODEL

3.1 Assumptions of the Interface Smeared Crack Model

The Interface Smeared Crack Model (ISCM) is designed to simulate the behavior of Mode-I* gradual joint-opening at interface joints. The model presented here is directly applicable to 2-D problems and with some minor modifications it can be extended to general 3-D problems. It is a simple and economical model based on the following assumptions:

(1) No relative shearing slip at the interface joints;

(2) gradual opening or closing, no impact phenomenon will occur;

(3) all nonlinear properties, e.g., material nonlinearities, are lumped at interface joints, so the remaining part of the structure is linear elastic;

(4) the strain energy released due to joint-opening is equivalent to the strain energy released by local material modifications on the non-crack structural topology;

(5) joint opening or reopening is indicated by tensile normal stress across the interface joint;

(6) joint closing or reclosing is indicated by compressive normal strain across the interface joint;

(7) complete joint opening will not necessarily fail the structure; the structural system will fail only due to divergence of the change in structural stiffness;

(8) only small displacement behavior of the structural system is considered;

---

* Mode-I cracking is the term used in fracture mechanics to describe the opening of a crack without any relative shearing slip, either in-plane or out-of-plane.

(9) the strain energy of an element in noncracked structural topology
with local material modifications is equivalent to the strain energy
stored in the element after the local pushing-back operation.

The ISCM retains all the advantages of a smeared crack model, but includes
a pushing-back operation to eliminate some of the disadvantages; it is
described in the following sections.

3.2 Description of the Interface Smeared Crack Model

In this section we will describe conceptually how the ISCM is
derived. This description is not intended to present the actual modelling
procedure, but to set forth the basic considerations in constructing the
ISCM. Let us start by examing a 2-D arch rib structure that is modelled
by finite elements (Fig. II-3(a)); only one element is used across the
thickness of the arch rib.

Now, when this arch rib is at its deformed position with the exact
joint-opening, it is at a condition of minimum potential energy
(Fig. II-3(b)). However, for the global solution, the ISCM requires a
noncracked structural configuration; therefore, we restore continuity as
follows: stretch the elements by pulling all the separated nodes back,
and piece them together pair by pair (Fig. II-3(c)). Obviously this
operation will add extra tensioning strain energy to the structural
system and this extra strain energy is computationally lumped at the
quadrature integration points of the elements. In order to release this
extra strain energy so that the structural system will remain at minimum
potential energy, the smeared crack modelling process suggests that local
material modifications be made at those quadrature integration points that
were strained artificially by the stretch and piece together operation.
In general, the local material modifications are applied at those quadrature
integration points located at the part of the interface that is opened.

Also they are made in such a way that the normal stresses, at those
quadrature integration points along the opened interface, will vanish,
in order to satisfy the stress boundary condition normal to the opened
interface. For this purpose, Lobatto Quadrature (Fig. II-2(d)), an
implicit boundary quadrature integration scheme, is used in the ISCM so
that the behavior of the interface joint along the element boundary
(Fig. II-3(b)) can be properly monitored. Now, we assume that the strain
energy released by local material modification at the quadrature integra-
tion points located along the opened interface, is equivalent to the
strain energy added to these quadrature integration points when the element
was undergoing the stretch and piece together operation. Therefore, the
local material modifications applied with the stretch and piece together
operation introduced no change of strain energy to the structural system,
if no other quadrature integration points altered their strain energy
during this operation.

But it is evident that the stretch and piece together operation will
not only add strain energy to those quadrature integration points located
along the opened interface, but also will strain other quadrature inte-
gration points in the element as well. Although this straining of other
quadrature integration points will not pose much change of strain energy
to the structural system as a whole, it nevertheless will influence the
stress variations within the element. Because no criteria can be used to
apply local material modifications to these other quadrature integration
points in the same way as to those quadrature integration points located
along the opened interface, we seek another approach involving performing
a second operation on the model after the global solution is obtained by
means of the general smeared crack model. The second operation is
intended to correct the stress variations within the element, it involves

releasing both the piecing together of paired nodes and the stretching
of the element by "pushing back" the nodes at the element level
(Fig. II-3(d)). Thus, the correct joint-opening at element boundaries
is obtained; that is, the correct element displacement vector is
produced. Then, the stresses can be evaluated using this correct element
displacement vector and the material moduli defined without any local
material modifications (except where compression softened material must
be considered). If the amount and direction of pushing back is correct,
we will reproduce the vanished normal stress condition that satisfies the
stress boundary condition at the opened interface, and every block
between two consecutive interface joints will be at its equilibrium
position. However, the correct amount and direction of pushing back are
hard to determine unless the exact solution is known beforehand. Also,
we feel that the equilibrium of the block between two consecutive inter-
face joints is a more important condition to satisfy than the stress
boundary condition at the opened interface, if both cannot be satisfied
at the same time.

The foregoing description indicates the general concept of how the
ISCM is to be constructed. The advantage of ISCM lies in the global
solution stage that requires no additional equations beyond those of the
continuous system and no redefinition of the structural topology; minimal
expenses are required,for the local pushing-back operations intended to
produce the correct local structural behavior, because they are done at
the element level.

3.3 Modelling Process

We now can proceed to detail the construction of ISCM. For computat-
ional purposes, we first have to specify the locations of the interface

joints as input information, realizing that the properties of ISCM are associated with quadrature integration points located along the interfaces. Then, the global response analysis is carried out, followed by determination of the material state of behavior. Because we assumed that all non-linearities of the structure are defined at interface joints, the material state determinations are checked on interface joints only. The Newton-Ralphson nonlinear iteration scheme is adopted to carry out the analysis. Therefore, after the state of joint-opening or joint-closing has been determined, the local material modifications are made appropriately for all quadrature integration points located along the interface. If the state of joint-opening has changed, new element stiffness matrices as well as new global stiffness matrix are formed. It is then that the pushing-back operations are performed element by element for each location where an opened interface is indicated. At this time, the opening width and opening ratio are evaluated, and stresses are computed at each quadrature integration point within the element. Finally, the internal resisting force is calculated and the unbalanced load vector is formed. Convergence tolerance is checked for each change of the global stiffness matrix, and the unbalanced load is carried over to the next iteration or next time step.

Details of the modelling procedure are presented in the following sections.

3.3.1 Interface Joint Locations and Lobatto Quadrature Integration

Interface joints are discrete precracked sections in the structure; they open at predefined locations and in predefined directions. Since all the nonlinearities are associated with the interface joints, in order for the state determinations to be performed on these predefined interfaces, we have to specify through input where the interface joints are located,

or, where the state determinations are to be carried out.

We have mentioned that the properties of ISCM are associated with element quadrature integration points that are located along the interfaces, and we are using ISCM to simulate the behavior of interface joints, therefore, it is natural to specify the location of an interface joint by giving element numbers and their quadrature integration points that are located along the interface. A convenient way to accomplish this kind of specification is by numbering the quadrature integration points that are associated with each element (Fig. II-2(d)). Thus, an interface joint is located by knowing the element numbers that it joins and the quadrature integration point numbers that its properties are associated with. The state determination for this interface joint then is performed on these integration points.

In order that interface joints can be located by such specifications, we need to use implicit boundary quadrature integrations which have the integration points along the boundaries of the element. Then, if the structure is discretized so that interface joints lie at boundaries of elements, the quadrature integration points will line up along the interfaces.

Lobatto quadrature is an implicit boundary quadrature integration scheme that has its integration points located at boundaries of the domain of integration, i.e., at boundaries of the element. The order of accuracy of the scheme is $2n-3$, where n is the number of integration points along a given line. Abscissas and weighting functions used with the scheme are as follows:

n	Abscissa	Weight
2	± 1	1
3	0	4/3
	± 1	1/3
4	$\pm 1/55$	5/6
	± 1	1/2
5	0	32/45
	$\pm\sqrt{3/7}$	49/90
	± 1	1/10

The Lobatto quadrature integration scheme has the highest precision among all implicit quadrature integration schemes.

3.3.2 State Determinations at Interface Joints

From the initial state of the structural system, we carry out the response analysis and find the current state nodal displacements. Then the state determination is performed on each quadrature integration point associated with interface joints, and local modifications are made on those quadrature integration points that have changed their state from the initial state.

3.3.2.1 Joint-Opening and Corresponding Local Material Modifications

For each quadrature integration point associated with the interface joints, we check its state of opening if it was closed. In general, a smeared crack model opens a quadrature integration point in its principal direction once its principal stress exceeds the tensile strength of the material. But in ISCM, the direction of joint-opening is predefined, that is, normal to the interface, and the tensile strength of material at the interface joint in the direction normal to the interface is zero. Therefore, the joint-opening state of any interface joint which is simulated

by ISCM, is determined by the tensile normal stresses at quadrature integration points located along the interface. At this time it must be recognized that stress continuity is not guaranteed across the element interface (26,29); the normal stress on one side of the interface may be in tension while it is in compression on the other side across the joint, therefore, a normal stress indicator has to be used for checking the state of joint-opening. The simplest method is to use the averaged normal stress across the joint as the normal stress indicator.

Once the normal stress indicator at a quadrature integration point along an interface is shown to be in tension, the interface joint will physically separate into two sides at that location and the normal stress indicator will be reduced to zero at that quadrature integration point. But with ISCM requiring noncracked structural topology, instead of actually splitting the joint into two sides, we apply a local material modification on that quadrature integration point in such a way that the corresponding normal stress indicator will vanish. This will yield a locally anisotropic material (the stiffness matrix is kept to be symmetric).

In order to modify the material properties, we have to make use of the assumed material constitutive law. Material behavior based on "equivalent uniaxial strain" is a simple yet fairly accurate constitutive model for the concrete (24,27,32,33). In general, it relates principal stress to the equivalent uniaxial strain while considering the effects of the stress state in other directions; but for our purpose, we simplify it a little further.

In general, the orthotropic stress-strain relationship in the direction normal to the interface, may be expressed as

$$\varepsilon_{nn} = \frac{\sigma_{nn}}{E_{nn}} - \nu_{ns} \frac{\sigma_{ss}}{E_{ss}} - \nu_{nt} \frac{\sigma_{tt}}{E_{tt}} \tag{3.1}$$

or,

$$\varepsilon_{nn} = \frac{\sigma_{nn}}{E_{nn}} \left(1 - \nu_{ns} \frac{\sigma_{ss}}{\sigma_{nn}} \frac{E_{nn}}{E_{ss}} - \nu_{nt} \frac{\sigma_{tt}}{\sigma_{nn}} \frac{E_{nn}}{E_{tt}}\right)$$

From this we may write:

$$\sigma_{nn} = \tilde{E}_{nn} \left(\nu_{ns}, \nu_{nt}, a_{sn}, a_{tn}, b_{ns}, b_{nt}\right) \cdot \varepsilon_{nn} \qquad (3.2)$$

where

$$a_{sn} = \frac{\sigma_{ss}}{\sigma_{nn}}$$

$$a_{tn} = \frac{\sigma_{tt}}{\sigma_{nn}}$$

$$b_{ns} = \frac{E_{nn}}{E_{ss}}$$

$$b_{nt} = \frac{E_{nn}}{E_{tt}}$$

$$\tilde{E}_{nn} = E_{nn}/(1 - \nu_{ns} a_{sn} b_{ns} - \nu_{nt} a_{tn} b_{nt})$$

For simplicity, we assume $(1 - \nu_{ns} a_{sn} b_{ns} - \nu_{nt} a_{tn} b_{nt})$ to be approximately constant; then $\tilde{E}_{nn}$ is a direct function of E_{nn} and we could directly relate σ_{nn} to ε_{nn} if the values $\tilde{E}_{nn}$ could somehow be supplied. Thus, the complex nonlinear relationship between σ_{nn} and ε_{nn} has been reduced to a simple form depending on empirical values of $\tilde{E}_{nn}$.

Now, in general, the local material modifications, on a quadrature integration point along an interface where it is opened, are performed on the material matrix associated with that quadrature integration point, in the direction normal to the interface. For 2-D plane stress or plane strain,

$$\underline{D}_n = \begin{bmatrix} 0 & 0 & 0 \\ 0 & E_{ss} & 0 \\ 0 & 0 & \beta G \end{bmatrix} \qquad (3.3)$$

where β is normally taken as 0.5. Then by coordinate transformations to

rotate $\underline{D}_n$, we obtain the Rectangular Cartesian Coordinates (RCC) expression $\underline{D}$, that is

$$\underline{D} = \underline{A}^T \, \underline{D}_n \, \underline{A} \tag{3.4}$$

where

$$\underset{\sim}{\varepsilon}_n = \underline{A} \, \underset{\sim}{\varepsilon}$$

$\underline{A}$ = Coordinate transformation matrix for strains

$$\underset{\sim}{\varepsilon}_n = <\varepsilon_{nn} \; \varepsilon_{ss} \; \gamma_{ns}>^T$$

$$\underset{\sim}{\varepsilon} = <\varepsilon_{xx} \; \varepsilon_{yy} \; \gamma_{xy}>^T \text{ in RCC}$$

$$\gamma_{ns} = \varepsilon_{ns} + \varepsilon_{sn}$$

$$\gamma_{xy} = \varepsilon_{xy} + \varepsilon_{xy}$$

The material matrix $\underline{D}$ is then used to form the element stiffness matrix contributions from this quadrature integration point.

3.3.2.2 Joint-Closure and Corresponding Local Material Modifications

For each quadrature integration point associated with interface joints, we check its state of closure if it was opened. The state of joint-closure is indicated by the compressive normal strain indicator, in the direction normal to the interface. As mentioned above, the indicator is an averaged value across the interface joint.

When the normal strain indicator at a quadrature integration point along an interface indicates that it is in compression, the interface joint will close at that location. The ISCM assumes that when the joint is closed, it resumes full strength of the material in all directions; that is, an isotropic material property is re-established at the closed quadrature integration point (unless compression damage has occurred).

Therefore, for any closed quadrature integration point, we have to check if accumulative compression damages has occurred. If so, the

material is softened according to the constitutive law employed, and in ISCM, this kind of material softening due to compression damage is considered permanent. The local material modification due to compression damage at a quadrature integration point is performed similarly to the method discussed in the previous section as follows.

Firstly, for a closed quadrature integration point located along an interface, we check its normal stress indicator. If the normal stress indicator at this quadrature integration point exceeds the material compressive strength $\sigma_{u,c}$, then the local material is softened according to the constitutive law adopted (say the elastic-perfectly-plastic rule) so that the normal stress indicator will be brought back to a value not to exceed $\sigma_{u,c}$. Thus, the local material modification is made on the material matrix associated with that quadrature integration point, in the direction normal to the interface. For 2-D plane stress or plane strain,

$$\underline{D}_n' = \begin{bmatrix} a_{uc}D_{11} & a_{uc}D_{12} & a_{uc}D_{13} \\ & D_{22} & D_{23} \\ \text{Symm} & & D_{33} \end{bmatrix} \qquad (3.5)$$

where

D_{ij} = (i,j) entry of isotropic material matrix of concrete

$a_{uc} = \sigma_{u,c}/\sigma_{nn}$, reduction factor of material compressive strength

σ_{nn} = normal stress indicator at the quadrature integration point normal to the interface.

Then, similarly applying the coordinate transformation to obtain the RCC expression of material matrix $\underline{D}'$,

$$\underline{D}' = \underline{A}^T \underline{D}_n' \underline{A} \qquad (3.6)$$

where

$\underline{A}$ = concrete transformation matrix for strains

$\underline{D}'$ = RCC representation of material matrix for compression softened

material.

Notice that the reduction factor a_{uc} is permanent and accumulative. The

material matrix $\underline{D}'$ is then used to form the contributions to the element

stiffness matrix from this quadrature integration point.

3.3.2.3 Pushing-Back Operation

In the general smeared crack modelling procedure, after the state of

opening or closure is determined and the corresponding local material

modifications are done, it proceeds to the global solution for the next

iteration or next time step. But as we mentioned earlier, due to the

incorrect element displacement vector of the noncracked structural

topology (that is, the element displacement vector produced by the stretch

and piece-together operation applied to the actual model of the element),

the stress variation within the element is not properly represented. To

correct this, we suggested that the pushing-back operation be done on the

element; that is, to produce the actual physical deformation of the

element by pushing-back the artificially pieced-together nodes that were

supposed to be splitted. Then the stresses within the element can be

calculated with this corrected element displacement vector, using the

original material moduli without any local material modifications (except

for those caused by compression damages).

The amount and direction of pushing back are hard to determine, yet

they are vital for reproducing the zero normal stress condition along the

opened interfaces and for equilibrating the block between two consecutive

interface joints. We consider that the global equilibrium condition of a

block is more crucial than satisfying local stress boundary conditions

along the opened interface; therefore, the pushing back operation will be

based on the global equilibrium and hope that the stress boundary condition will be satisfied approximately at the same time.

The direction of pushing back can be reasonably taken as normal to the interface. The amount of pushing back is found by numerical experiment so that the block between two consecutive interface joints will be in the best equilibrium position after pushing back. At the same time the normal stress indicators along the opened interface should be small.

The amount of pushing-back is computed at each quadrature integration point located along the opened interface, and ISCM suggests it to be given by

$$d_w = \alpha_\omega \cdot \varepsilon_{nn} \cdot (J_{ij})^{1/m} \tag{3.7}$$

where

α_ω = empirical coefficient obtained by numerical experiments; it depends on the geometry and aspect ratio of the element being considered

ε_{nn} = normal strain indicator computed at this quadrature integration point, positive for tension

J_{ij} = Jacobian of this quadrature integration point

m = reference spatial dimension of the element being considered.

Notice that the pushing back operation is done at the nodes of the element, yet the amount of pushing back is computed at the quadrature integration points; therefore, the quadrature integration points have to be located to coincide with the nodes of the element. Now, since the element displacement vector is normally expressed in RCC components, in order to modify the element displacement vector by the pushing back operation we have to find the RCC components of d_w in Eq. (3.7). This can be obtained through

the normal direction cosines at the quadrature integration point where d_w is computed. Subtracting the RCC components of d_w from the corresponding element displacements of the degrees of freedom associated with this nodal point, we obtain the corrected element displacement vector. The stresses and strains within the element are computed using this corrected element displacement vector, using material moduli that are not modified for joint-opening but are only modified for compression damages. The internal resisting forces of the element can be evaluated by the standard finite element formula,

$$\underset{\sim}{f}_I^{(e)} = \iiint_{V^{(e)}} \underline{B}^{(e)^T} \underset{\sim}{\sigma}^{(e)} \, dV^{(e)} \qquad (3.8)$$

where

$V^{(e)}$ = domain of the element e

$\underset{\sim}{\sigma}^{(e)}$ = vector of elemental stresses

$\underline{B}^{(e)}$ = strain-displacement transformation matrix for element e.

3.3.2.4 Unbalanced Load and Convergence Tolerance Criteria

After the current state of response has been determined and the pertinent response quantities have been evaluated, we proceed as in a general nonlinear response analysis, to form the structural unbalanced load and check the solution for convergence to see if iteration within the same step is necessary.

There are two approaches generally being used in nonlinear iterations. One is to carry over the unbalanced load without iteration in the same time step as long as the time intervals are chosen reasonably small; the other is to perform nonlinear iteration until the convergence tolerance criteria are met, and then proceed to next step without carry over of any unbalanced load.

For our particular case, we have to combine these two approaches, namely, to do nonlinear iterations within the time step until the convergence tolerance criteria are met and also to carry over the unbalanced load to the next step after convergence. The reason is that it is only suitable in our case to check the convergence on the change of stiffness of the structural system, while due to the pushing back operation, which is not guaranteed to be consistent with variations of structural stiffness, the unbalanced load may still be large after convergence of the stiffness of the structural system.

Therefore, for the convergence tolerance check, we proceed as follows, using Newton-Ralphson nonlinear iterations:

(1) before updating the stiffness matrix, compute $\underset{\sim}{q}_i = \underline{K}_i \underset{\sim}{U}$;

(2) after updating the stiffness matrix, compute $\underset{\sim}{q}_{i+1} = \underline{K}_{i+1} \underset{\sim}{U}$;

(3) check $\varepsilon_p > ||\underset{\sim}{q}_{i+1} - \underset{\sim}{q}_i||_2$;

where

$\underset{\sim}{U}$ = current incremental structural displacement response,

$\underline{K}_i$ = structural stiffness used to compute $\underset{\sim}{U}$, i.e., before the current state determinations,

$\underline{K}_{i+1}$ = structural stiffness updated after the current state determinations which are based on $\underset{\sim}{U}$,

i = current iteration number, i = 0,1,2,---

ε_p = specified convergence tolerance (input),

and, the unbalanced load at the end of ith iteration $\underset{\sim}{R}_i^u$ is,

$$\underset{\sim}{R}_{i+1}^u = \underline{K}_i \underset{\sim}{U} - \underset{\sim}{f}_i^I + \underset{\sim}{f}_{i-1}^I \qquad\qquad (3.9)$$

where

$$\underset{\sim}{f}_i^I = \underset{e}{\Sigma} \; \underset{\sim}{f}_I^{(e)}$$ assembled internal resisting forces at the end

of ith iteration, after state determinations. $\underset{\sim}{f}_I^{(e)}$ is defined

in Eq. (3.8)

$\underset{\sim}{f}_{i-1}^I$ = assembled internal resisting forces at the end of

$(i-1)^{th}$ iteration, that is, at the beginning of ith iteration.

For $i=0$, $\underset{\sim}{f}_{i-1}^I = \underset{\sim}{0}$.

If the convergence tolerance check on the change of stiffness does not satisfy the specified criterian, the unbalanced load is carried over to the next iteration, otherwise, the unbalanced load is carried over to next time step. The change of stiffness will converge when the pattern of joint-opening of the structural system is stabilized, and normally this convergence can be achieved fairly quick. The structure is considered to have failed if the norm of the change of stiffness is diverging, that is, if the structural system fails to stabilize its joint-opening mechanism.

3.3.3 Computations of Opening Width and Opening Ratio

At the end of each time step, in addition to element stresses and nodal displacements, it would be interesting to evaluate specific joint quantities such as opening width, that is how wide is the joint opened, and opening ratio, that is how deep does the opening penetrate into the joint.

If we recall how the ISCM is constructed to simulate the joint-opening behavior of an interface joint, it would not be difficult to observe that the sum of the amount of pushing back of all elements at the interface joint is just the opening width of the joint at that location. Because the amount of pushing back is calculated at quadrature integration

points along the interface which coincide with nodal points of the element, the opening width will also be evaluated at those quadrature integration points. If a joint is located at a fixed support, its opening width is just the amount of pushing back calculated at the quadrature integration point of its adjacent element. If a joint is located elsewhere, its opening width will be the sum of the amounts of pushing back calculated at the quadrature integration points of each element which is adjacent to this joint (Fig. II-4(a)).

Thus, the opening width D_w at one end of an interface joint is,

$$D_w = \sum_e d_w \tag{3.10}$$

where d_w is defined in Eq. (3.7).

The opening ratio of an interface joint is defined as the fraction of the joint that is opened compared to the entire interface joint length. It is found by locating the zero opening width along the joint, but because the opening widths along an interface joint are calculated at discrete quadrature integration points, the location of the zero opening width along the joint must be found by interpolation. To be consistent with the quadratic isoparametric FEM formulation, the opening width is computed as follows (Fig. II-4(b)); firstly the location of the zero opening width is established as:

$$D_w = 0 = N_1 \, D_{w_1} + N_2 \, D_{w_2} + N_3 \, D_{w_3} \tag{3.11}$$

where D_{w_1}, D_{w_2}, D_{w_3} = opening widths at quadrature integration points; positive for opening, negative for closing in compression

$$N_1 = 1/2(1+\xi)-1/2(1-\xi^2), \ 1 \le \xi \le -1$$

$$N_2 = 1/2(1-\xi)-1/2(1-\xi^2)$$

$$N_3 = 1-\xi^2$$

Eq. (3.11) can be rewritten as,

$$a\xi^2 + b\xi + c = 0 \tag{3.12}$$

where

$$a = 1/2(D_{W_1} + D_{W_2})-D_{W_3}$$

$$b = 1/2(D_{W_1} - D_{W_2})$$

$$c = D_{W_3}.$$

Solving Eq. (3.12) for ξ. If ξ falls outside of the range of -1 and +1, the joint is either completely opened or completely closed; the specific condition is indicated by whether D_{W_3} is positive or negative. If ξ falls between -1 and +1, the opening ratio ρ_ω is obtained as,

$$\rho_\omega = 1/2(1+\xi_i\xi) \tag{3.13}$$

where

$\xi_i = -1$, if ρ_ω is defined as positive when the joint is opened at the end $\xi = +1$,

$\xi_i = +1$, if ρ_ω is defined as positive when the joint is opened at the end $\xi = -1$.

4. COMPUTER IMPLEMENTATION AND NUMERICAL EXAMPLES

A computer program NDARCH (37) was developed to carry out the non-linear dynamic response analysis of an arch rib with a joint-opening nonlinear mechanism, using step-by-step numerical integration. The response quantities are output on a tape file and then go through a postprocess plotting program. The results of the nonlinear response, such as stresses, strains, displacements, opening widths and opening ratios, are plotted against time.

4.1 Computer Implementation

The ISCM for simulating the joint-opening behavior is implemented in NDARCH, and an economical step-by-step numerical integration scheme for general nonlinear dynamic response analysis is also included. Their implementations are described briefly in the following sections.

4.1.1 An Economical Step-by-Step Numerical Integration

The step-by-step numerical integration scheme proposed here uses a simple way of forming the unbalanced load vector, to minimize storage requirements and computational effort.

To evaluate dynamic response of a structural system, the equation of motion to be integrated may be expressed:

$$\underline{M}\,\ddot{\underline{U}} + \underline{C}\,\dot{\underline{U}} + \underline{K}\,\underline{U} = \underline{F} - \underline{M}\,\underline{r}\,v_g \qquad (4.1)$$

where

$\underline{M}$ = global mass matrix of the structural system

$\underline{C}$ = global damping matrix of the structural system

$\underline{K}$ = global stiffness matrix of the structural system

$\underline{F}$ = external nodal load vector, including both static and dynamic

forces

$\underline{r}$ = pseudostatic influence coefficient matrix

$\ddot{\underline{V}}_g = <\ddot{V}_{gx} \ \ddot{V}_{gy} \ \ddot{V}_{gz}>^T$ ground accelerations vector

$\ddot{\underline{U}}, \dot{\underline{U}}, \underline{U}$ = structural responses: acceleration, velocity and displacement respectively.

For dynamic equilibrium at time t_{n+1}:

$$\underline{M} \ \ddot{\underline{U}}_{n+1} + \underline{C} \ \dot{\underline{U}}_{n+1} + \underline{K}_{n+1} \ \underline{U}_{n+1} = \underline{P}_{n+1} \tag{4.2}$$

where

$\underline{P}_{n+1} = \underline{F}_{n+1} - \underline{M} \ \underline{r} \ \ddot{\underline{V}}_{gn+1}$

$\underline{K}_{n+1}$ = structural stiffness matrix at time t_{n+1}

$\underline{M}, \underline{C}$ are assumed constant throughout the response history.

The step-by-step numerical integration scheme gives,

$$\ddot{\underline{U}}_{n+1} = a_0(\underline{U}_{n+1} - \underline{U}_n) - a_2\dot{\underline{U}}_n - a_3\ddot{\underline{U}}_n$$

$$\dot{\underline{U}}_{n+1} = a_1(\underline{U}_{n+1} - \underline{U}_n) - a_4\dot{\underline{U}}_n - a_5\ddot{\underline{U}}_n \tag{4.3}$$

where a_0 through a_5 are integration constants. These vary with the different numerical integration schemes used, such as the Newmark Method, Wilson θ-Method or α-Method (28,35,38,39). Substituting Eq. (4.3) into Eq. (4.2) and rearranging it, we have

$$[a_0\underline{M} + a_1\underline{C} + \underline{K}_{n+1}] \ \underline{U}_{n+1} = \underline{P}_{n+1} + \underline{M}(a_0\underline{U}_n + a_2\dot{\underline{U}}_n + a_3\ddot{\underline{U}}_n) +$$

$$\underline{C}(a_1\underline{U}_n + a_4\dot{\underline{U}}_n + a_5\ddot{\underline{U}}_n) \tag{4.4}$$

Now, for nonlinear dynamic response analysis using the Newton-Ralphson Method, we solve Eq. (4.4) for $\underline{U}_{n+1}$ with known $\underline{U}_n$, $\dot{\underline{U}}_n$, $\ddot{\underline{U}}_n$ and P_{n+1}. Because $\underline{K}_{n+1}$ is unknown, the solution can only be obtained by iterations.

The nonlinear dynamic iteration scheme used here can be illustrated by 2 iterations:

Let $\hat{\underline{K}}_{ID} = a_0\underline{M} + a_1\underline{C}$

$$\underline{Q}_{n+1} = \underline{P}_{n+1} + \underline{M}(a_0\underline{U}_n + a_2\dot{\underline{U}}_n + a_3\ddot{\underline{U}}_n) + \underline{C}(a_1\underline{U}_n + a_4\dot{\underline{U}}_n + a_5\ddot{\underline{U}}_n)$$

First iteration:

(1) $\hat{\underline{K}}_{n,0} = \hat{\underline{K}}_{ID} + \underline{K}_{n,0}$, where $\underline{K}_{n,0} = \underline{K}_n$

(2) Solve $\hat{\underline{K}}_{n,0}\, \underline{v}_{n+1,0} = \underline{R}_0^U$, where $\underline{R}_0^U = \underline{Q}_{n+1}$

By numerical integration scheme:

$$\ddot{\underline{v}}_{n+1,0} = a_0(\underline{v}_{n+1,0} - \underline{U}_n) - a_2\dot{\underline{U}}_n - a_3\ddot{\underline{U}}_n$$

$$\dot{\underline{v}}_{n+1,0} = a_1(\underline{v}_{n+1,0} - \underline{U}_n) - a_4\dot{\underline{U}}_n - a_5\ddot{\underline{U}}_n$$

(3) Form the unbalanced load $\underline{R}_1^U = \underline{P}_{n+1} - \underline{M}\,\ddot{\underline{v}}_{n+1,0} - \underline{C}\,\dot{\underline{v}}_{n+1,0} - \underline{f}_0^I$

where $\underline{f}_0^I$ = internal resisting force corresponding to $\underline{v}_{n+1,0}$

Utilizing the integration scheme, we could have

$$\underline{R}_1^U = \underline{Q}_{n+1} - \hat{\underline{K}}_{ID}\,\underline{v}_{n+1,0} - \underline{f}_0^I$$

or, from (1) and (2),

$$\underline{R}_1^U = \underline{K}_{n,0}\,\underline{v}_{n+1,0} - \underline{f}_0^I$$

(4) By the Newton-Ralphson Method, update the current stiffness matrix

$\underline{K}_{n,1}$ and apply the stiffness convergence tolerance check

$$\varepsilon_p > ||\underline{K}_{n,1}\,\underline{v}_{n+1,0} - \underline{K}_{n,0}\,\underline{v}_{n+1,0}||_2$$

(5) Carry over unbalanced load $\underline{R}_1^U$; if the convergence is not yet achieved

do the next iteration.

Second iteration:

(1) $\hat{\underline{K}}_{n,1} = \hat{\underline{K}}_{ID} + \underline{K}_{n,1}$

(2) Solve $\hat{\underline{K}}_{n,1}\, \Delta\underline{v}_1 = \underline{R}_1^U$ (4.5)

Update $\underline{v}_{n+1,1} = \underline{v}_{n+1,0} + \Delta\underline{v}_1$

Here we observe that superimposing Eq. (4.5) with Eq. (4.4), we have

$$[\hat{\underline{K}}_{ID} + \underline{K}_{n,1}] \, \underline{v}_{n+1,1} = \underline{Q}_{n+1} + \underline{K}_{n,1}\underline{v}_{n+1,0} - \underline{f}_0^I \qquad (4.6)$$

or,

$$\underline{Q}_{n+1} = \hat{\underline{K}}_{ID}\underline{v}_{n+1,1} + \underline{K}_{n,1}\Delta\underline{v}_1 + \underline{f}_0^I \qquad (4.7)$$

(3) Form unbalanced load $\underline{R}_2^u = \underline{P}_{n+1} - \underline{M} \, \ddot{\underline{v}}_{n+1,1} - \underline{C} \, \dot{\underline{v}}_{n+1,1} - \underline{f}_1^I$

By the numerical integration scheme:

$$\ddot{\underline{v}}_{n+1,1} = a_0(\underline{v}_{n+1,1}-\underline{U}_n)-a_2\dot{\underline{U}}_n - a_3\ddot{\underline{U}}_n$$

$$\dot{\underline{v}}_{n+1,1} = a_1(\underline{v}_{n+1,1}-\underline{U}_n)-a_4\dot{\underline{U}}_n = a_5\ddot{\underline{U}}_n$$

The unbalanced load then becomes

$$\underline{R}_2^u = \underline{Q}_{n+1} - \hat{\underline{K}}_{ID}\underline{v}_{n+1,1} - \underline{f}_1^I$$

and using Eq. (4.7), we have

$$\underline{R}_2^u = \underline{K}_{n,1}\Delta\underline{v}_1 - \underline{f}_1^I + \underline{f}_0^I$$

(4) Update current stiffness $\underline{K}_{n,2}$ and apply the stiffness convergence tolerance check $\varepsilon_p > ||\underline{K}_{n,2}\underline{v}_{n+1,1}-\underline{K}_{n,1}\underline{v}_{n+1,1}||_2$.

(5) Carry over unbalanced load $\underline{R}_2^u$; if it has not yet converged do next iteration.

Thus, the nonlinear dynamic iteration procedure for the time step from t_n to t_{n+1} can be summarized as follows:

(i) Form $\hat{\underline{K}}_{ID} = a_0\underline{M} + a_1\underline{C}$

for Rayleigh damping $\hat{\underline{K}}_{ID} = (a_0 + a_1a_M) \, \underline{M} + a_1a_K\underline{K}_I$

where $\underline{C} = a_M\underline{M} + a_K\underline{K}_I$

$\underline{K}_I$ = initial stiffness matrix of the system

(ii) For each iteration $i = 0,1,2,\text{---}N$, do the following:

(1) Form $\hat{K}_{n,i} = \hat{K}_{ID} + K_{n,i}$, where $K_{n,0} = K_n$

(2) Solve $\hat{K}_{n,i} \Delta v_i = R_i^u$

where $R_0^u = P_{n+1} + M(a_0 U_n + a_2 \dot{U}_n + a_3 \ddot{U}_n) + C (a_1 U_n + a_4 \dot{U}_n + a_5 \ddot{U}_n)$.

(3) Update $v_{n+1,i} = v_{n+1,i-1} + \Delta v_i$, with $v_{n+1,(-1)} = 0$

Form f_i^I corresponding to $v_{n+1,i}$

(4) Update current stiffness matrix $K_{n,i+1}$, according to Newton-Ralphson Method.

(5) Form unbalanced laod

$$R_{i+1}^u = K_{n,i} \Delta v_i - f_i^I + f_{i-1}^I, \text{ with } f_{(-1)}^I = 0$$

(6) Apply stiffness convergence tolerance check

$$\varepsilon_p > ||K_{n,i+1} v_{n+1,i} - K_{n,i} v_{n+1,i}||_2$$

Carry over unbalanced load R_{i+1}^u

(7) If it has not yet converged, go to (1) for next iteration $i+1$.

(8) If it has converged, define initial conditions for next time step $t_{n+1} \sim t_{n+2}$:

$$U_{n+1} = v_{n+1,N}$$

$$\ddot{U}_{n+1} = a_0(U_{n+1} - U_n) - a_2 \dot{U}_n - a_3 \ddot{U}_n$$

$$\dot{U}_{n+1} = a_6(U_{n+1} - U_n) - a_7 \dot{U}_n - a_8 \ddot{U}_{n+1}$$

and proceed to next time step.

It should be noticed in Eq. (4.6), that in general the formation of $\underline{K}_{n,i+1}$ and $\underline{f}_i^I$ are consistent, and that $\underline{K}_{n,i+1} \underline{v}_{n+1,i} = \underline{f}_i^I$. However, in the ISCM that involves the pushing back operation, the formation of $\underline{K}_{n,i+1}$ and $\underline{f}_i^I$ are not consistent; therefore $\underline{K}_{n,i+1} \underline{v}_{n+1,i} - \underline{f}_i^I \neq \underline{0}$, and the remaining residual will be accumulated in the unbalanced load vector which must be carried over to the next iteration or next time step. This is the reason why we proposed in ISCM that the convergence should be checked not on the unbalanced load, but rather on the change of the structural stiffness.

4.1.2 Implementation of State Determination of ISCM

In the nonlinear dynamic response analysis, the state determination is the central phase of the response analysis. After the current structural displacements have been updated, we have to go through the state determination phase in order to find the current structural internal resisting force, and the current state of material properties which will be used to form the current structural stiffness matrix.

Since the state determination procedure varies with different nonlinear mathematical models, in the following we will only describe the computational procedure for state determination of ISCM.

We have assumed that all the nonlinearity of the structural system is lumped at the interface joints whose behavior is simulated by ISCM, and the properties of ISCM are associated with the quadrature integration points of the elements located along the interfaces. Therefore, state determinations are to be performed on those quadrature integration points of elements associated with ISCM.

For easier data preparation, the locations of precracked interface joints are input by specifying the element numbers and node numbers of the elements; then the computer program internally converts these

specifications to the corresponding quadrature integration point numbers associated with each element. After that, the attention is focused on every element and each of its quadrature integration points is examined whether or not it is associated with ISCM and locate at an interface. If it is at interface, the state determination is done on it, otherwise the procedure skips to the next quadrature integration point or next element. It is a special feature of ISCM that the joint-opening nonlinear mechanism is embedded in the properties of finite elements in the actual computational procedure. Notice that the joint-opening is in the predefined direction normal to the interface, thus the normal direction cosines associated with those quadrature integration points of the elements along the interfaces need to be precalculated.

The computational algorithm for state determination of ISCM is summarized as follows:

(A) Compute the current normal stress indicators and normal strain indicators

    (a) For element number 1,2,--NEL, do:

        (1) Read in current element displacements

    (b) For quadrature integration points associated with this element, do:

        (1) If this quadrature integration point is not at interface, skip;

        (2) Compute normal stress and normal strain at this quadrature integration point of this element, according to current elemental displacements and current material properties; the outward normal from the element is taken as positive.

    (c) For element number 1,2,---NEL, do:

(d) For quadrature integration points associated with this element, do:

(1) If this quadrature integration point is not at interface, skip;

(2) Average normal stress and normal strains across the inter-face joints, and use the averaged quantities as normal stress indicators and normal strain indicators. For this to be done, we need to use the input specifications of the locations of interface joints to link the two quadrature integration points located at the same point.

(B) State determination on every quadrature integration point of every element

(a) For element number 1,2,---NEL, do:

(1) Read in current element displacements.

(b) For quadrature integration points associated with this element, do:

(1) If this quadrature integration point is not at interface, skip.

(2) If this quadrature integration point was opened, check if its current normal strain indicator is in compression (negative):

(i) If the normal strain indicator is in compression:

1. Change the state index of this quadrature integration point to closure.

2. Check if it is damaged in compression:

If $\sigma_{nn} > \sigma_{u,c}$, compressive damage occurred, compressive strength of the material reduced by an accumulative factor $a_{uc} = \sigma_{u,c}/\sigma_{nn}$ (see Eq. (3.5)).

(ii) Otherwise, compute the amount of pushing back (see Eq. (3.7)) and modify current element displacements. For 2-D case, $d_w = \alpha_w \cdot \epsilon_{nn} \cdot \sqrt{J_{i_j}}$, where $\alpha_w = 0.94$, chosen by numerical experiments.

(3) If this quadrature integration point was closed, check if its current normal stress indicator is in tension (positive):

(i) If the normal stress indicator is in tension:

1. Change the state index of this quadrature integration point to opening.

2. Compute the amount of pushing back and modify current element displacement. For 2-D case, $d_w = \alpha_w \cdot \epsilon_{nn} \cdot \sqrt{J_{i_j}}$, where $\alpha_w = 0.94$.

(ii) Otherwise, check if it is damaged in compression:

If $\sigma_{nn} > \sigma_{u,c}$, compressive damage occurred, compressive strength of the material reduced by an accumulative factor $a_{uc} = \sigma_{u,c}/\sigma_{nn}$.

(4) Modify the material matrix according to the current state index of this quadrature integration point, and update the current element stiffness contributions from this quadrature integration point.

(c) Update the structural stiffness matrix by assembling the current element stiffness matrix of this element into global stiffness matrix.

(d) For quadrature integration points associated with this element, do:

(1) Find the material matrix for this quadrature integration point; it is not modified for joint opening but only for accumulative compressive damages.

(2) Compute element stress at this quadrature integration point according to the element displacements which are modified by the pushing back operation.

(3) Compute element stresses at this quadrature integration point according to the material matrix obtained in (1) and strains obtained in (2).

(4) Compute the internal resisting force contributions from the stresses at this quadrature integration point, and update element internal resisting force vector.

(e) Update the structural internal resisting force by assembling the current element internal resisting force vector of this element into the global structural internal resisting force vector.

Now, after the global structural stiffness matrix and global structural internal resisting force vector are updated according to the current state of the structural system, the nonlinear dynamic response analysis can be continued to form the unbalanced load vector and then to apply the convergence tolerance check.

4.2 Numerical Examples

To illustrate the validity of ISCM for simulating joint-opening nonlinear behavior, several numerical examples are carried out. Firstly, a block contact problem is investigated in detail which demonstrates that the pushing back operation is crucial for obtaining reasonable global response as well as local responses. Then, the response of an arch rib with precracked interfaces is studied. Its compression failure mechanism

is investigated under static loadings, and its nonlinear dynamic response to simulated earthquake ground motions is analyzed.

4.2.1 Block Contact Problem

A block contact problem specially designed to demonstrate the efficiency of the ISCM modelling process is presented in Figures II-5 through II-10. The results are compared with those obtained from the computer program FEAP(34), which uses node-on-node contact elements to monitor the joint-opening behavior.

The structure consists of two plane stress blocks, 10 in^2 each, with a joint between them, the system is subjected to pure bending which opens the interface joint; it is a pure mode-I joint-opening. In ISCM, two 9-node plane stress elements were used to model each block, whereas by FEAP the block system was discretized into 4-node linear plane stress elements. (Fig. II-5).

In Fig. II-6, we show the displacement solutions due to different approaches. It is apparent that using ISCM without pushing back operation will yield results unacceptable even for the global response quantities such as displacements, the error in this case is approximately 50%. On the other hand, ISCM with pushing back operation has demonstrated good agreement with the solution obtained by FEAP, which uses a node-on-node contact element. In this case of simple pure bending, the displacements calculated by FEAP can be considered to have good accuracy. It shows that the joint-opening penetrates through points b, c, d; after the bending only points e,f are still in contact.

Figure II-7 illustrates the equilibrium condition of a block due to various approaches, all the nodal forces in the horizontal direction (X_1-direction) are negligible and are not shown. The vertical nodal

forces shown in Figures II-7(a) and II-7(b) are equivalent internal resisting nodal forces while the vertical nodal forces in Fig. II-7(c) are external loads and reactions. Figure II-7(c) shows that the block is in perfect equilibrium condition and that the contact forces at points e and f are accurate. Comparing Fig. II-7(b) with Fig. II-7(c), the nodal forces differ by a large amount, the contact forces at points e and f of Fig. II-7(b) are far off, its nodal reaction force at point a is also too small and the nodal forces at opened points b, c, d are too big. If we compare Fig. II-7(a) with Fig. II-7(c), we can see they are in reasonable agreement, especially in the contact forces at points e,f and the reaction at point a. Therefore, although Fig. II-7(b) shows a better equilibrium condition than that of Fig. II-7(a), ISCM with pushing back operation should be regarded as a better model than that without pushing back operation. The residual error in Fig. II-7(a) can be reduced to a minimal value by choosing the amount and direction of pushing back properly. The values shown in Fig. II-7(a) are due to pushing back in the direction normal to the interface by the amount $0.94 \ \varepsilon_{nn} \sqrt{J_{i_j}}$, which is defined in Eq. (3.7).

Figure II-8 through II-10 compare the variations of stresses within the block. They show again the importance of including the pushing back operation in ISCM for obtaining reasonable local stresses, and thus also strains. Figure II-9(a) shows excessive shear stress along the opened interface, this is due to the residual nodal forces (Fig. II-7(a)) that were not eliminated by the pushing back operation. Figure II-10(b) shows a perfect normal stress condition along the opened interface, yet its σ_{22} variations within the block are not appealing. The residual normal stress along the opened interface in Fig. II-10(a) implies that the amount and/or direction of pushing back is not optimal; the remaining normal

stress along the opened interface in Fig. II-10(c) is due to the finite element discretization error. It should be realized that the stresses obtained from FEAP as shown in Figures II-8(c), II-9(c) and II-10(c) are the results of interpolation using the linear stress variation properties of the 4-node linear element employed. The stresses output from FEAP were at the Gaussian quadrature integration points of each element; then stresses at the corners of the elements were found by interpolation or extrapolation and plotted in Figures II-8(c), II-9(c) and II-10(c) for comparison.

It is observed that in this static case under constant loadings the joint-opening at one end has increased the normal compressive stress σ_{22} at the other end of the interface joint by approximately 100% (if there were no interface joint between the blocks, the maximum compressive stress σ_{22} at point f under this pure bending would be 12 psi). Thus, the stress redistribution due to the joint opening at one end of the interface will tend to amplify the normal compressive stress at the other end, if the section forces at the interface section are not reduced. We can conclude the same for the normal strains.

It also should be noticed that, although the amounts of pushing back at opened points along the interface are very small compared to the dimensions of the block (approximately 0.01%), this operation has made a major improvement in the response solutions, such as displacements and stresses.

4.2.2 Compression Failure Mechanism of Arch Ribs

An arch rib representing a horizontal section of an arch dam is depicted in Fig. II-11; the interface joints of the arch rib coincide with the contraction monolith joints of the arch dam.

In this section, we will investigate the compression failure
mechanism of an arch rib. To expedite the failure of the structure, the
stabilizing gravity load is removed and the structure is subjected to horizontal
static concentrated nodal loads only. The total response of the arch
rib will be studied in the next section when it is subjected to both
static gravity and dynamic loadings.

The compression failure of the arch rib will start with compressive
damages at corners of arch rib blocks. When the compressive damages
continue to intensify and extend, the local material softens accumulatively
until it reaches a point where it completely loses its strength. The
arch rib will then collapse due to material failure.

Figure II-12 illustrates this compression failure mechanism. Fig.
II-12(a) shows an arch rib subjected to static concentrated nodal loads
acting in the X_1-direction. The loadings are large enough to fail the
structure. We examine the material properties at three critical locations,
as marked in Fig. II-12(a) by solid squares. We choose to see the pro-
gressive softening of Young's Modulus in the direction normal to the
interfaces at chosen locations. Figures II-12(b), (c) and (d) show
the progressive reduction of Young's Modula with nonlinear iterations,
where E_n represents the current Young's Modulus in the direction normal
to the interface and $E_{n,0}$ represents the original value of E_n. We have
assumed there are shear keys between the blocks. It is evident that due
to the loadings applied, the arch rib will deform in antisymmetric form,
and the three locations we are interested in will all be in compression,
but the rate of material softening due to compressive damages, with
respect to iteration number, may not be identical at all three locations.
As shown in the figures, the normal Young's Modulus E_n is reduced to a very
small or negligible magnitude at each point at the end of the seventh

iteration. This means that the structure has almost no strength to resist the loadings at the end of the seventh iteration.

Therefore, the criterion of compression failure of arch ribs can be established by examining the softening of material strength, or equivalently, by checking the reduction of stiffness of the system. If the stiffness shows continuing softening that is never stabilized, it can be expected that the structural system is going to fail.

4.2.3 Nonlinear Dynamic Response Analysis of Arch Rib

The arch rib depicted in Fig. II-11 now is subjected to earthquake excitations, using the NS component of the El Centro 1940 accelerogram with the peak acceleration amplified to 0.6 g. Due to gravity load, the structure is relatively much more stable with regard to vertical ground motion, and the joint-opening behavior would not be manifested under vertical ground motion unless the peak acceleration is increased to around 1.0 g. Therefore, in the following only the gravity load and the horizontal ground acceleration will be considered. With this loading we will expect minor compressive damages at joint-1 and joint-3.

Figures II-13 through II-16 show the calculated dynamic responses of the arch rib. Three cases are plotted for comparison, namely, one with all joints active (solid line), another, a linear continuum structure without any interface joints (dashed line), and the other with only joints 1, 3, 6 and 8 active (broken line). Because of the loadings imposed, the structure will vibrate in an antisymmetric pattern. Joints 1, 3, 6, and 8 are expected to open more than joints 2, 4, 5, and 7; therefore, the results shown by the broken line, where joints 2, 4, 5, and 7 are sealed and the results where all joints are active (solid line) are expected to be similar. In all the figures, initial offsets are due to the static gravity load.

In Figure II-13(a), the larger displacement amplitude at node 23 due to the joint-opening nonlinear mechanism is clearly shown. The peak amplitude of the solid line has increased by approximately 19% compared to the dashed line and by 15% compared to the broken line. The similarity between solid line and broken line results is evident. The period elongation due to softening of the structure because of joint-opening also is apparent. The large initial offset in the vertical displacement of node 23, shown in Fig. II-13(b) is the static gravity load effect. The amplitude magnification and period elongation of the joint opening results are also shown there, but to a less degree than in Fig. II-13(a) because the ground moves in the horizontal direction only. The horizontal displacement of node 14 in Figure II-13(c) is similar to that in Fig. II-13(a), with amplitude magnification for the solid line of 35% and for the broken line of 30%. Figure II-13(d) shows the varying width of joint-opening at the extrados of joint-3; it is the sum of the amounts of pushing back at that corner of both elements 2 and 3. Note that the maximum amount of opening width throughout the response history is approximately 0.2% of the length of the interface joint, and approximately 0.05% of the length of its adjacent block.

Figures II-14 and II-15 show the normal stresses and normal strains respectively, at the extrados and intrados of joints 1 and 3. For both the solid line and broken line cases, the tensile normal stresses at joints 1 and 3 should vanish because they are active, but it is clear from Fig. II-14, excessive tensile normal stresses exist during the response history. This implies that the pushing back operation employed here is not optimal, and indicates the need for further research to find optimal direction of pushing back. When the block geometry varies, the optimal amount of pushing back may not be very sensitive to the geometry of the

block. In Figs. II-14 and II-15, it is evident that the tensile normal stresses and strains shown by the dashed line (continuum case) are larger than those of the other two cases as they should be. Figure II-15 shows that the peak compressive normal strains of dashed line are larger than those of the other two cases at the intrados of joints 1 and 3, yet smaller at the extrados; thus, demonstrates that joint-opening at the intrados increases the compressive normal strains at the extrados, but that joint-opening at the extrados reduces the compressive normal strains at the intrados. It was noted in section 4.2.1 that joint-opening at one end of the interface joint will increase the compressive normal strain at the other end of the joint, but that was for the case of static constant loading. Under dynamic loading, because of the relative motion of two blocks away from each other, the inertia effects apparently reduce the compressive loadings exerted upon the interface between these two blocks, and thus reduce the compressive normal stresses and strains at this interface. This is the case when the arch moves away from the center of curvature which causes a net reduction of the compression force that is acting on the interface section. When the arch moves in towards the center of curvature, the opposite effect is produced; that is, the resultant section force is increased. It is observed that material yielding occured for the solid line and broken line cases due to compressive damage at the extrados of joint-1 as shown in Fig. II-14(c) at time t = 0.22 second. The maximum compressive normal stress cannot exceed the compressive strength of the material at the interface joints $\sigma_{u,c}$ = 26.5 psi except for the dashed line case, where the material is assumed to be infinitely linear elastic. Therefore, at the extrados of joint-1, although the normal compressive strain shown by the dashed line is smaller than that of the other two cases (which is consistent with the behavior indicated above) the

normal compressive stress is larger because the material yielded for the other two cases. In Figs. II-14 and II-15, it is also shown clearly that the joint-opening nonlinear mechanism has elongated the period of vibrations.

Figure II-16 shows the opening ratio at joints 1 and 3; the positive opening-ratio indicates that the joint-opening occurred at the extrados edge. It is evident in both joints 1 and 3 that the joint-opening penetrated into the joint by more than 70%; in joint 1 the penetration was 78%, and in joint 3 its deepest penetration was 74%. At joint 1 the joint-opening was quickly restrained when the ground motion died out, but at joint-3 it continued even after the ground motion stopped. The rocking motion of the two adjacent blocks against the interface is clearly depicted in Fig. II-16.

5. REMARKS AND FURTHER DEVELOPMENTS

The ISCM for simulating the behavior of a joint-opening nonlinear mechanism as illustrated in the previous chapters, can be extended easily to the modelling of monolith contraction joint opening behavior in the 3-D dynamic response analysis of general arch dams. The only requirement is that boundary quadrature integration points of the elements be located at the interface joints. It should be clear now that the main reason for this is that the local material modifications of the ISCM must be done at the boundary quadrature integration points of the elements that are associated with the ISCM. The other quantities of interest, such as normal stress indicators, normal strain indicators and the amount of pushing back do not have to be calculated at quadrature integration points as long as they can be computed accurately at the required locations.

Because of the increased complexity and cost involved in a 3-D response analysis, we feel it would be beneficial to refine the current 2-D ISCM before undertaking a 3-D case. Improvements are needed especially with regard to the computation of the optimal direction and amount of pushing back, to better normal stress and normal strain indicators, and, if possible, to include the capability of simulating relative slipping of two blocks at an interface. One may even further elaborate the ISCM, in the energy sense, by studying how the global response of the system is affected by a local material modification done on a particular quadrature integration point of an element. After such refinements of the current 2-D ISCM, we could make some realistic correlation studies with the experimental results reported previously (30).

In the following we shall discuss some possible refinements and extensions of the 2-D ISCM:

(1) Direction and amount of pushing back

From Figures II-14 and II-15, it has been shown that excessively large tensile normal stresses and strains remained after the pushing back operation, where the direction of pushing back was taken as normal to the interface and the amount of pushing back was 0.94 $\varepsilon_{nn}\sqrt{J_{i_j}}$ (as defined in Eq. (3.7)). Therefore, it is clear that the direction and amount of pushing back are not optimal for this case, compared with the studies presented in section 4.2.1. It is believed that the poor results in Figs. II-14 and II-15 with regard to the remaining tensile normal strain and stress after pushing back is mainly due to the improper direction of pushing back. A better direction of pushing back may be along the surface of each element.

(2) Number of numerical quadrature integration points

One of the biggest concerns when we extend the response analysis into 3-D is the cost. For economic reasons we cannot maintain a large number of quadrature integration points. Therefore, different quadrature integration schemes in different directions may have to be adopted. Using the Lobatto quadrature integration scheme in the arch direction is deemed necessary in order to have quadrature integration points at the interface; however, in both the cantilever direction and the upstream-downstream direction, a Gaussian quadrature integration scheme could be employed. The problem remaining for further investigation, then, is how should the material matrix associated with any quadrature integration point at the interface be modified when the normal stress indicator at locations other than the quadrature integration points indicate that opening occurred.

(3) Normal stress and strain indicators

Besides the necessity of properly selecting the locations where the indicators are to be set, an inherent problem with finite element solutions is the stress and strain discontinuity across the element interface, due to the discretization error. The inconsistency of stress and strain values across the interface makes it difficult to set consistent stress and strain indicators at the interface. Averaged stress and strain across the interface are the simplest indicators that can be established, but they leave room for improvement. The traction associated with dynamic equilibrium along the element boundary at the interface could be a good stress indicator.

(4) Simulation of relative slipping (mode-II cracking)

We still could use the same basic concept applied as a "shear and piece-together operation" and "release the bond and shearing-back operation". The problems to be investigated would include establishing criteria for initiation of relative slipping. For example, the slipping might occur when the shear stress at the interface exceeds the value given by Coulomb's friction law. Also, to be studied are computation of the amount of shearing back to satisfy stress boundary conditions at the interface for portions both in contact and freed, and evaluation of the equilibrium of adjacent blocks. Other considerations similar to those involved in mode-I cracking should be examined for the small displacement range.

(5) Cantilever cracking and crushing

Joint-opening in the arch direction may have a major influence on the stress state in the cantilever direction. As mentioned earlier, the arches softened due to joint-opening will amplify the deflection

of the structure, thus will increase the deflection of the cantilever monoliths. This increased deflection in the cantilever will possibly increase the tensile cantilever stress and cause the cantilever cracks. Also, it was indicated that the joint-opening in the arch direction may increase the compressive arch stress at extrados, by Poisson effect, this will also increase the compressive cantilever stress and possibly lead to the cantilever crushing. The general smeared crack model in the literature could be directly adopted for simulating the cracking behavior of cantilever monoliths.

It is clear that the nonlinear dynamic response analysis of arch dams, including contraction monolith joint opening, cantilever cracking and other material nonlinearities is far from complete. Although it is not necessary to seek an analytical model that can predict the nonlinear dynamic response to extreme precision, much more research is needed to have a reasonable understanding of the arch dam response when it goes into the nonlinear range under intensive dynamic loadings.

6. CONCLUSIONS

A model for simulating the mode-I joint-opening nonlinear mechanism is presented in the previous chapters, namely, Interface Smeared Crack Model (ISCM). It is a simple and economical model based on the smeared crack model, but a special pushing-back operation is introduced mainly to improve the local structural responses, such as variations of stresses and strains. This operation nevertheless has also improved the global structural behavior, the displacements.

Because of smaller number of equations needed, the advantages and savings in computational effort of ISCM, as compared with most interface joint models proposed in the literature up to date, are evident. Moreover, an economical step-by-step numerical integration scheme is also proposed, which reduced much computational cost in the nonlinear dynamic iterations, by a cheaper way of forming unbalanced load vector as compared with most nonlinear dynamic iteration schemes used to date (38,39).

The accuracy of ISCM in predicting local and global structural responses is studied in detail on a block-contact problem, and the results are shown to be excellent for the case studied. Then, a complete nonlinear dynamic response analysis of an arch rib with interface joints is carried out. Detailed discussions on the behavior of the arch rib subjected to static gravity load and to horizontal earthquake ground motions are shown, and finally, some comments on the improvement of ISCM and its further developments are discussed.

For the costly computational effort in nonlinear dynamic response analysis of arch dams, the proposed ISCM has provided an efficient and economical way to simulate the contraction joint opening behavior, also because of the similarity in nature, the cracking of cantilever monoliths can be included in the ISCM very easily, with these advantages, the ISCM

proposed herein is potentially the best suitable approach for simulating nonlinear dynamic response of arch dams considering both contraction joint opening and cracking of cantilever monoliths.

JOINT-OPENINGS

$\ddot{u}_{gx}$
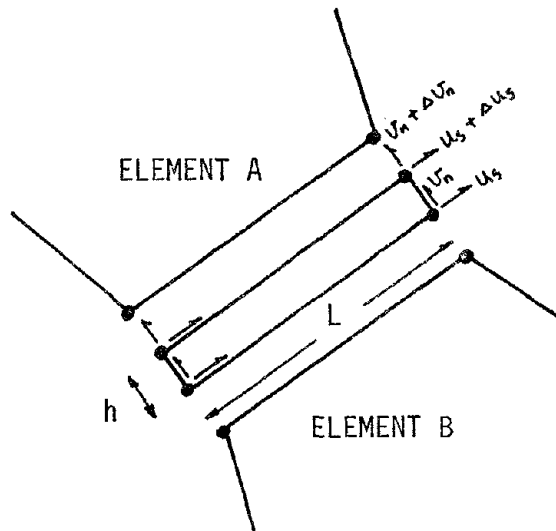
$\ddot{u}_{gy}$

$\ddot{u}_{gz}$
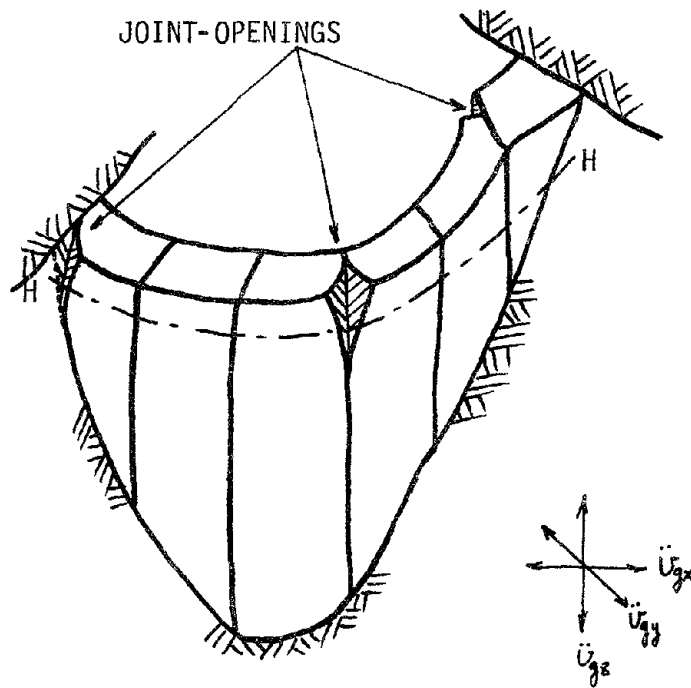
(a) MONOLITHS AND JOINTS
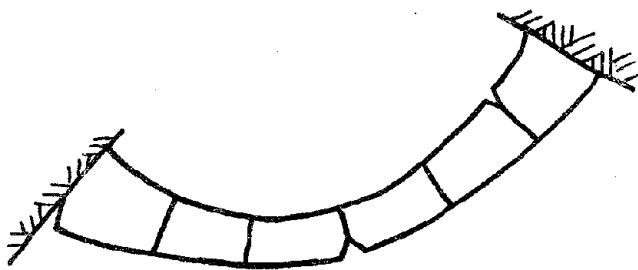
(b) HORIZONTAL SECTION H--H

FIG. II-1 ARCH DAM AND ARCH RIB

NODE-ON-NODE SPRING ELEMENT   NODE-ON-NODE CONTACT ELEMENT
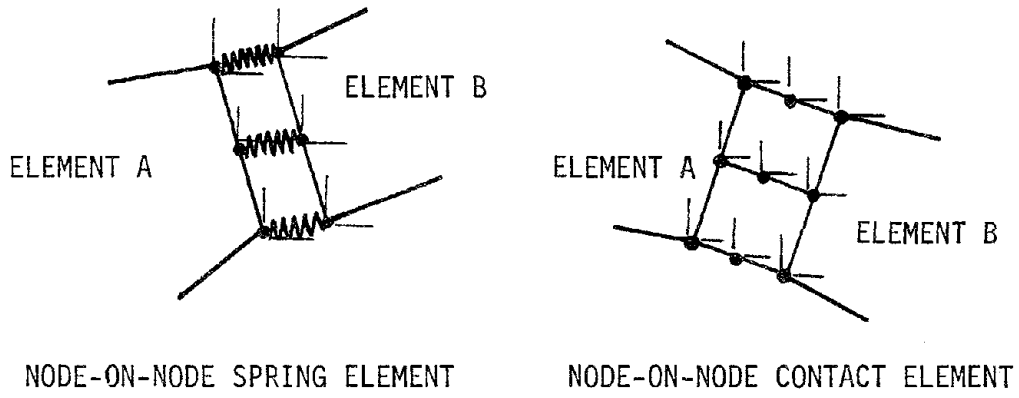
(a)

(b) JOINT ELEMENT

FIG. II-2 MODELS FOR INTERFACE JOINT SIMULATION

58

INTEGRATIONS

CRACK

9-NODE ELEMENT

SMEARED INTO TRIBUTARY REGION

INTEGRATIONS

CRACK

9-NODE ELEMENT

SMEARED THROUGHOUT THE ELEMENT

(c) SMEARED CRACK MODEL

LOBATTO QUADRATURE (3x3)
INTEGRATIONS

9-NODE ELEMENT
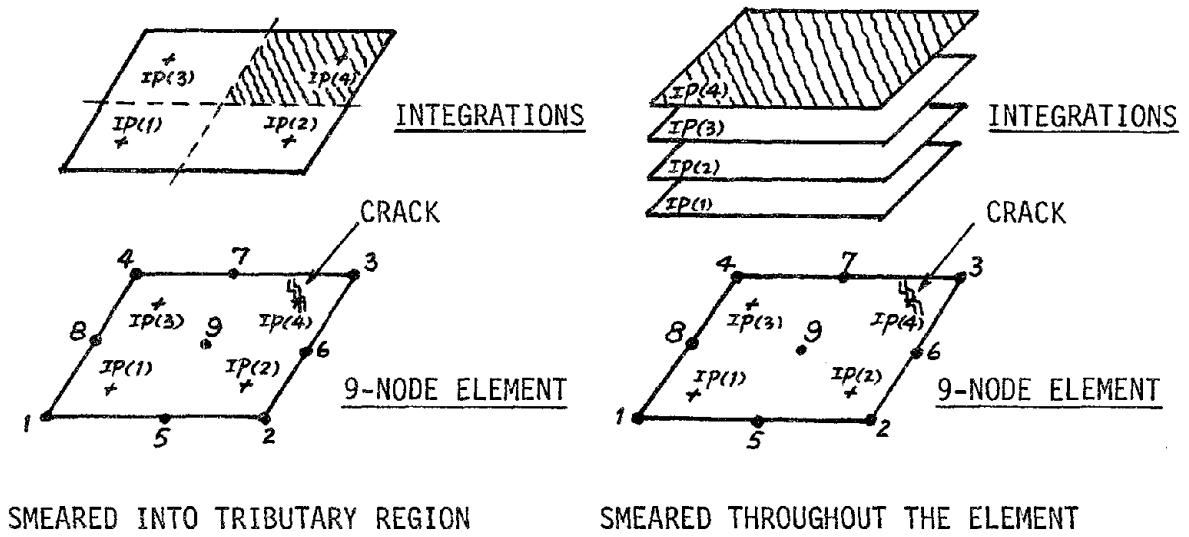
CRACK

CRACK
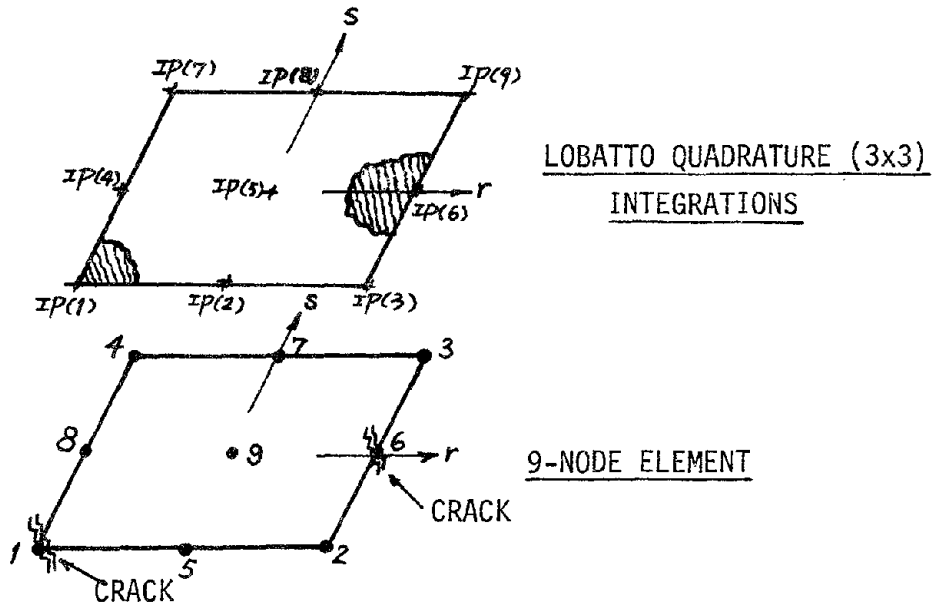
(d)

FIG. II-2 (Cont.) MODELS FOR INTERFACE JOINT SIMULATION
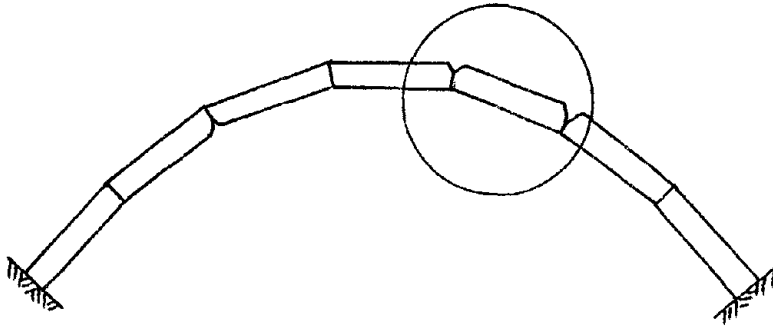
(a) FINITE ELEMENT MODEL FOR AN ARCH RIB
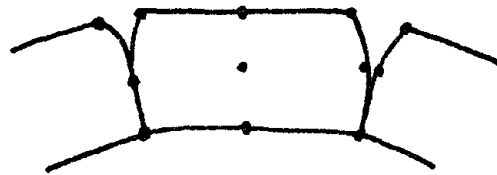
(b) INTERFACE JOINT-OPENING AT ELEMENT BOUNDARY
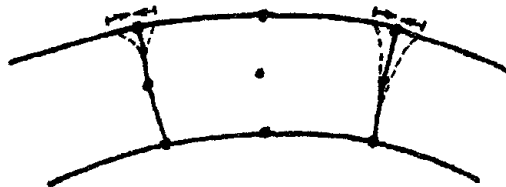
(c) STRETCH AND PIECE TOGETHER OPERATION
    FOR GLOBAL SOLUTION
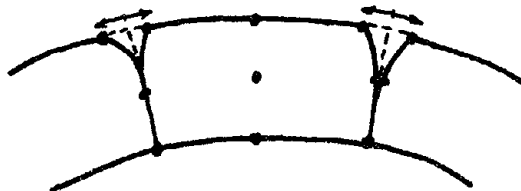
(d) PUSHING-BACK OPERATION AT ELEMENT LEVEL

FIG. II-3 ISCM MODELLING PROCESS
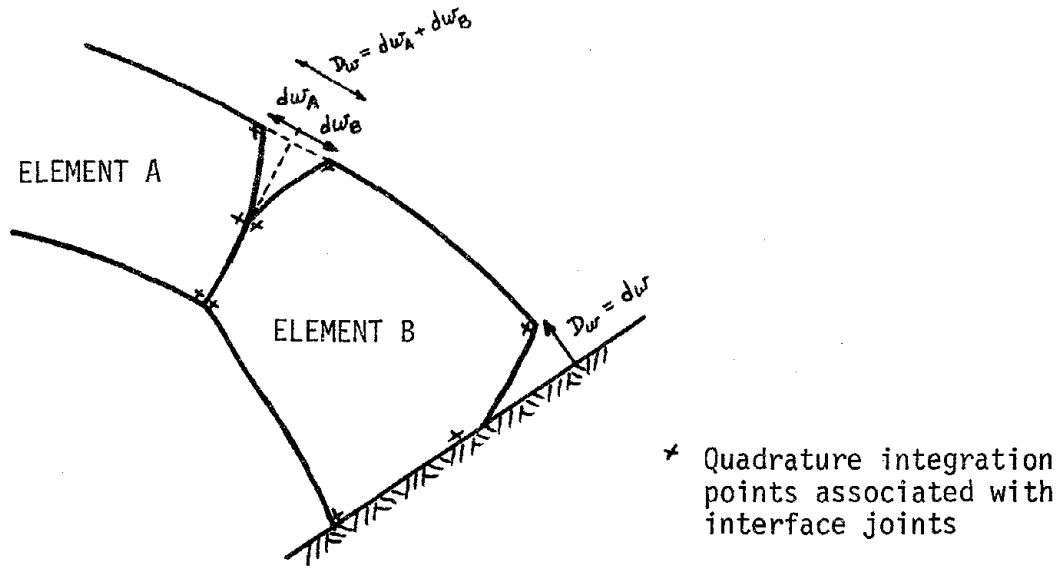
(a) OPENING WIDTH OF INTERFACE JOINTS

$\ast$ Quadrature integration points associated with interface joints
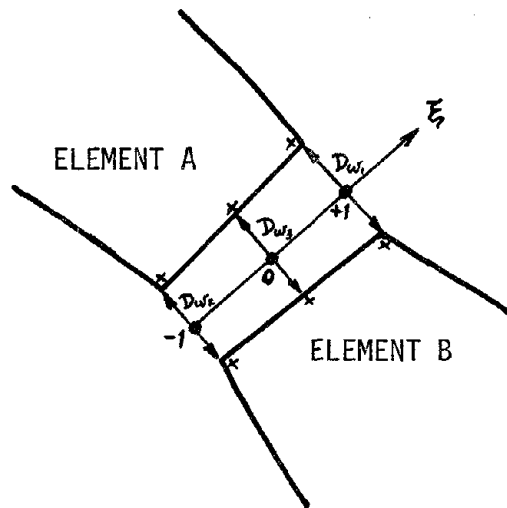
(b) OPENING RATIO OF INTERFACE JOINTS

FIG. II-4 OPENING WIDTH AND OPENING RATIO OF INTERFACE JOINTS
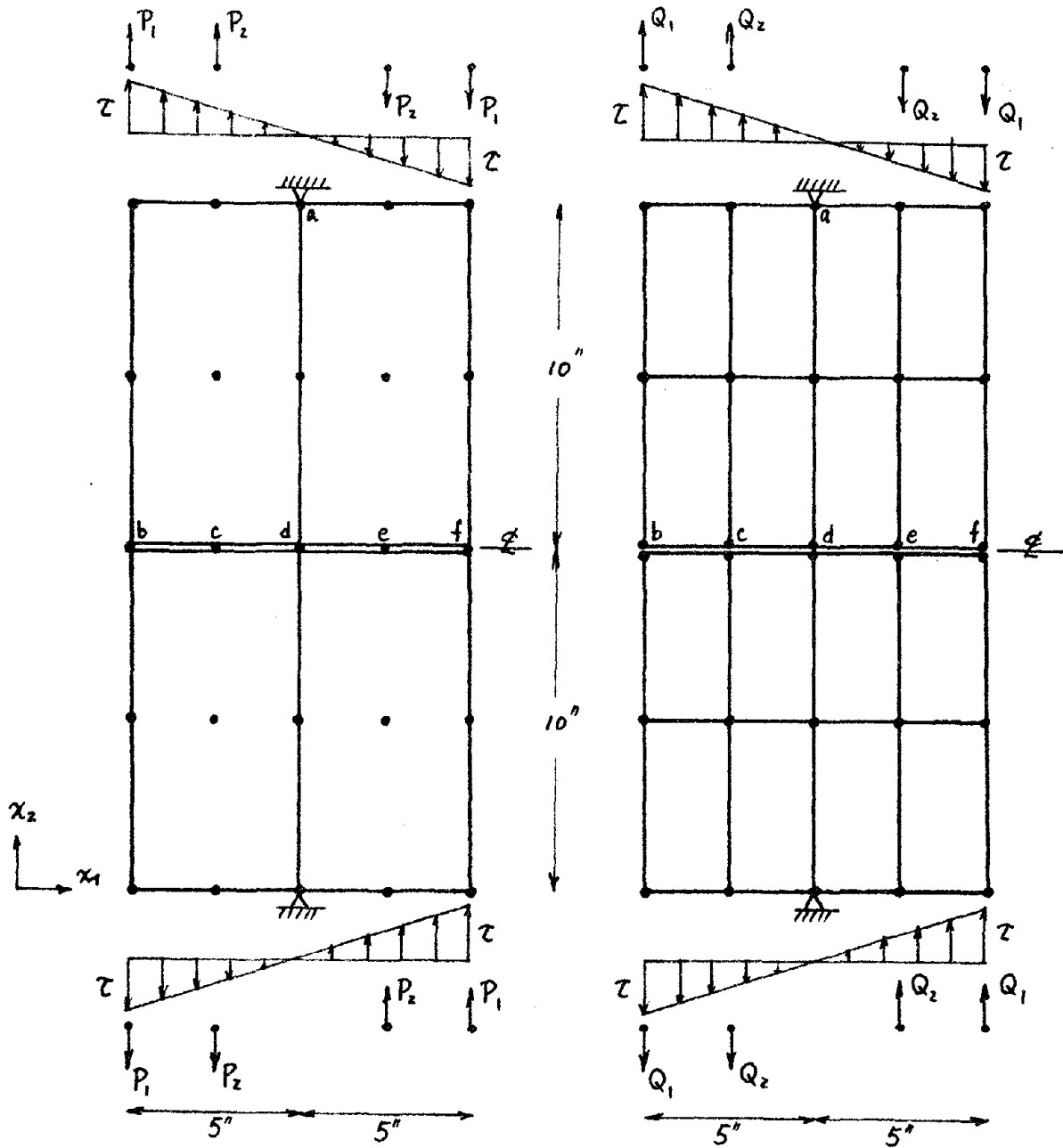
(a) FE MESH FOR NDARCH (37)   (b) FE MESH FOR FEAP (34)

Boundary traction applied τ = 12 psi
Equivalent nodal loads P_1 = 10 lb ; P_2 = 20 lb
                           Q_1 = 12.5 lb ; Q_2= 15 lb
Young's modulus E=4.0x10⁵ psi
Poisson's ratio ν=0.21
Plane stress elements
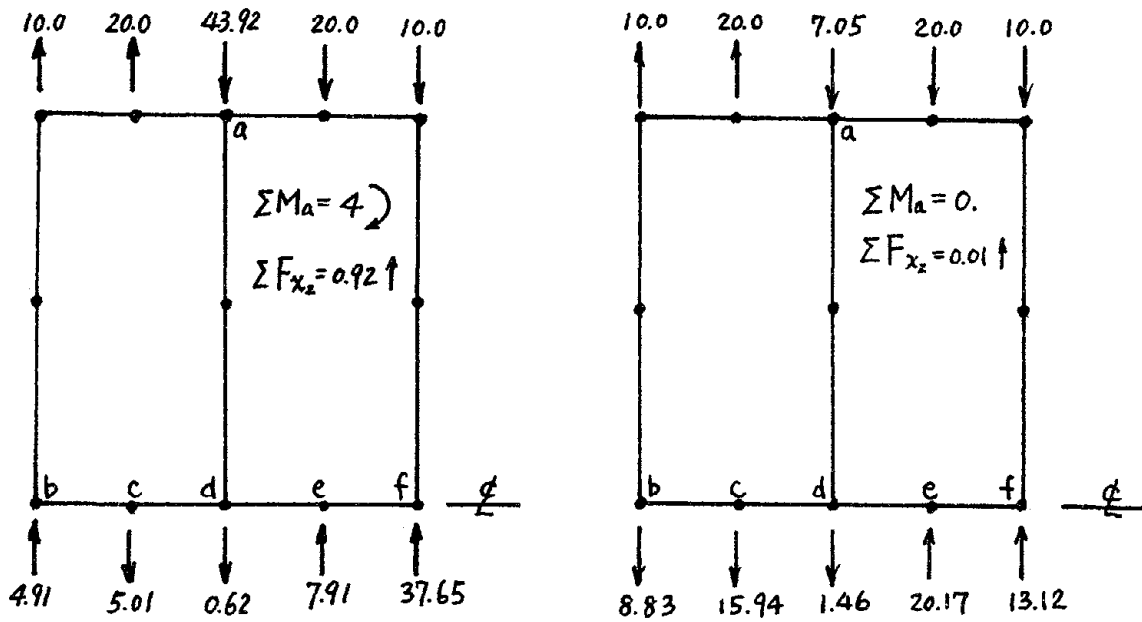
FIG. II-5 BLOCK CONTACT PROBLEM SUBJECTED TO PURE BENDING

ISCM with pushing-back operation
ISCM without pushing-back operation
Solution from FEAP (34)

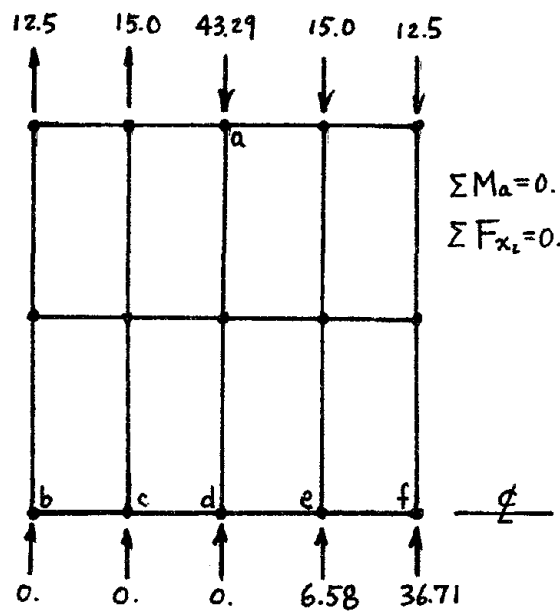Displacement scale 1.0×10^{-3} in
Mesh scale 2.5 in
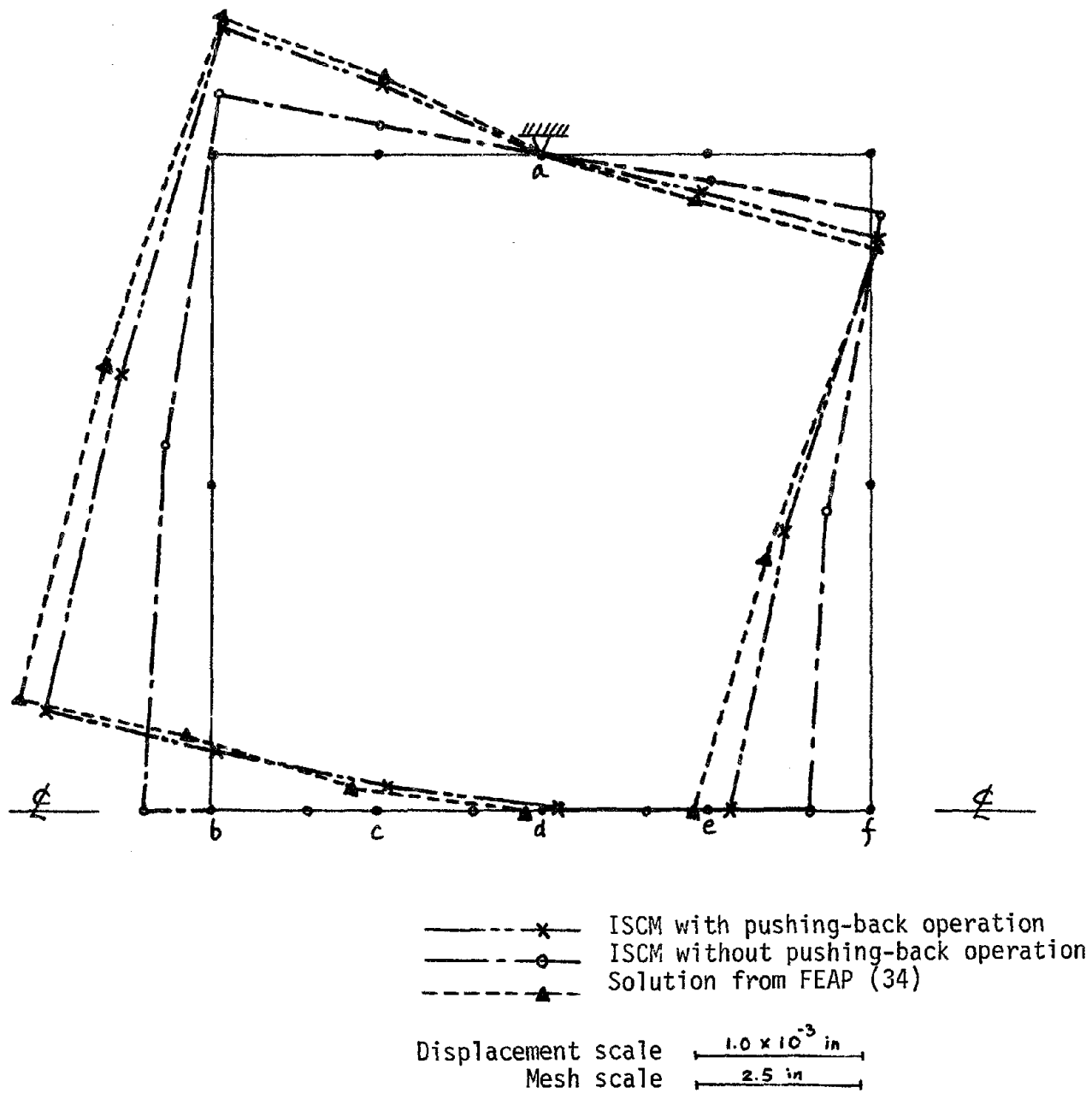
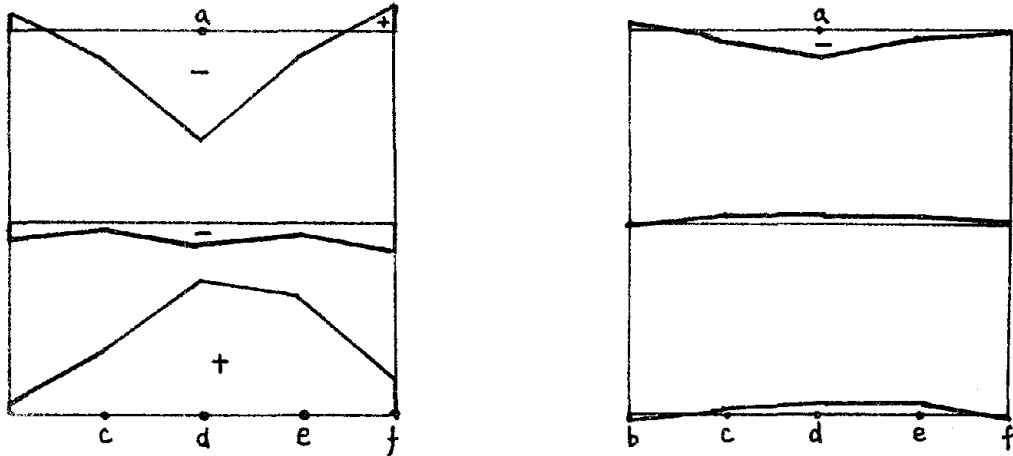FIG. II-6 DISPLACEMENT SOLUTION FOR BLOCK CONTACT PROBLEM

(a) ISCM WITH PUSHING-BACK OPERATION   (b) ISCM WITHOUT PUSHING-BACK OPERATION
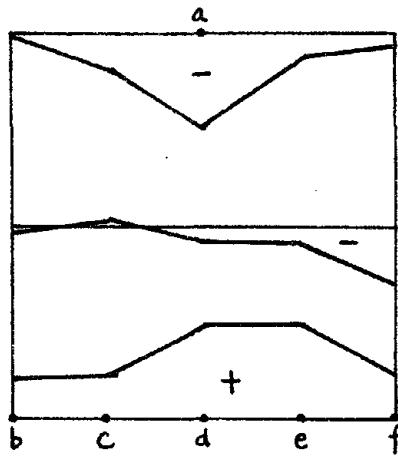
(c) SOLUTION FROM FEAP (34)

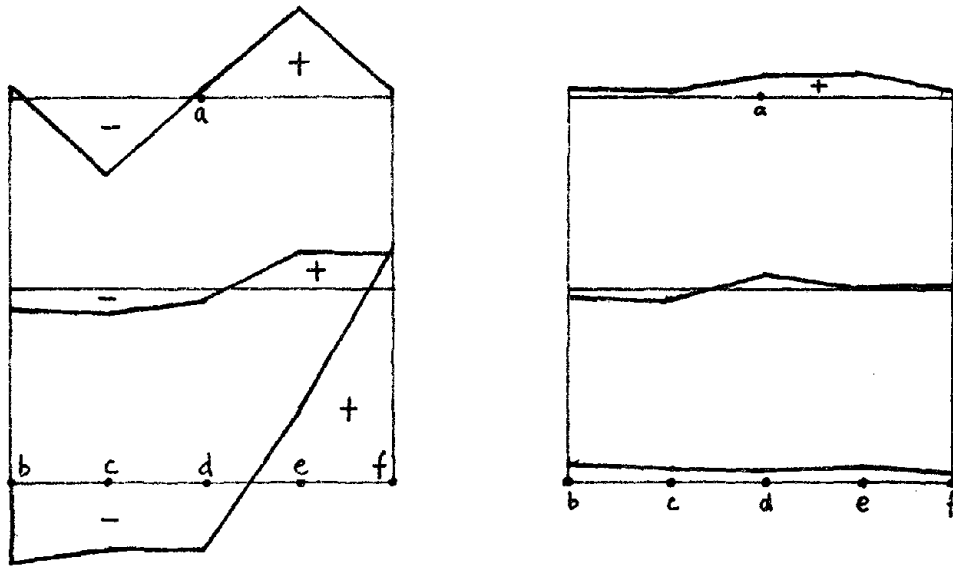FIG. II-7 EQUILIBRIUM CONDITION OF A BLOCK

(a) ISCM WITH PUSHING-BACK OPERATION   (b) ISCM WITHOUT PUSHING-BACK OPERATION
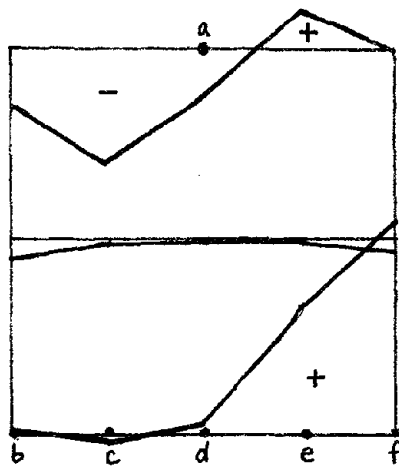
(c) SOLUTION FROM FEAP (34)

Stress scale
10 psi

FIG. II-8 VARIATIONS OF σ_{11}

(a) ISCM WITH PUSHING-BACK OPERATION (b) ISCM WITHOUT PUSHING-BACK OPERATION

(c) SOLUTION FROM FEAP (34)

Stress scale

$10\ psi$

FIG. II-9 VARIATIONS OF τ_{12}

(a) ISCM WITH
    PUSHING-BACK
    OPERATION

(b) ISCM WITHOUT
    PUSHING-BACK
    OPERATION

(c) SOLUTION FROM FEAP(34)

Stress scale

20 psi

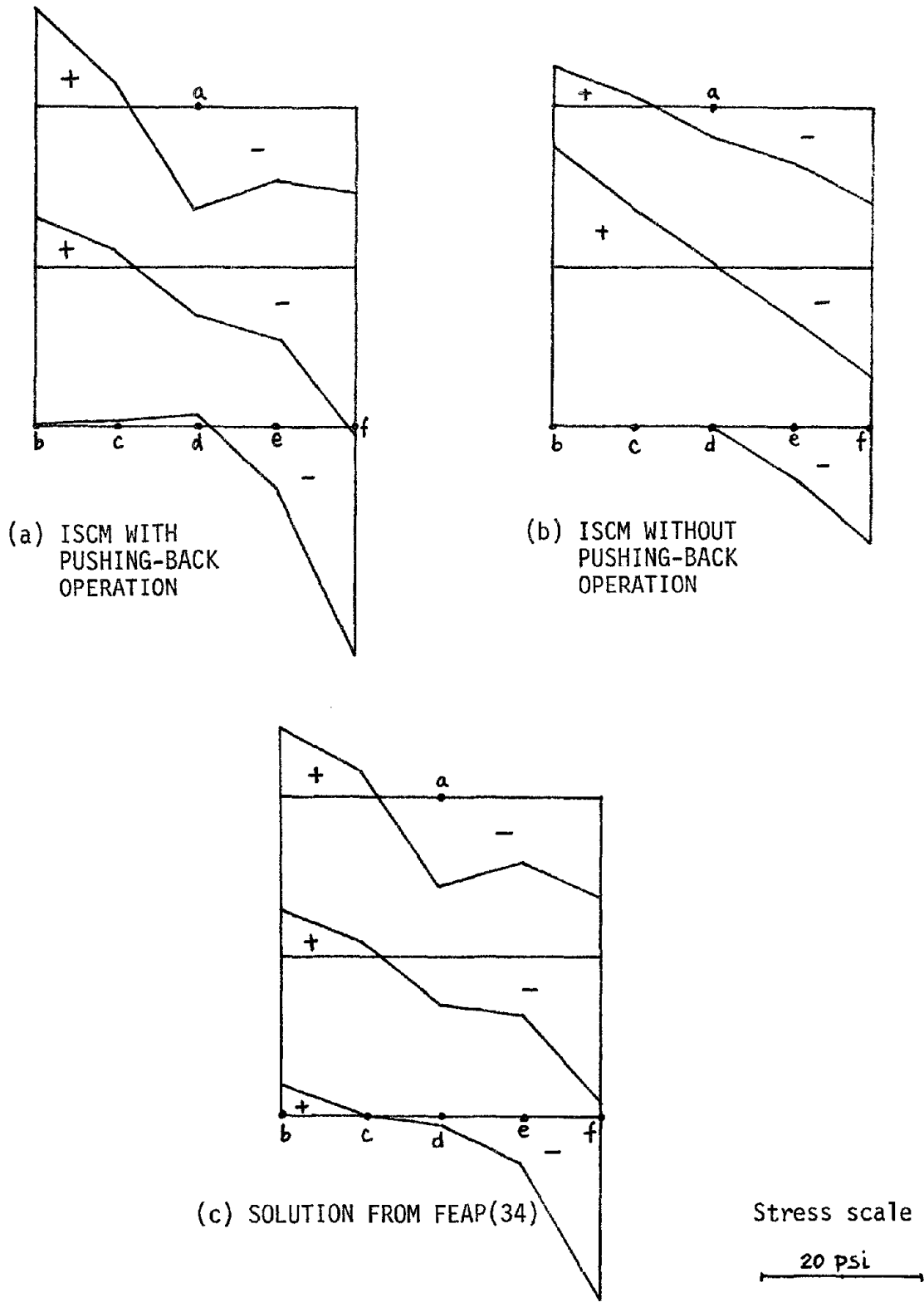FIG. II-10 VARIATIONS OF σ_{22}

Mesh scale $\overline{\phantom{12\frac{3}{4}}}$ *12 ¾ in.*

4: Joint number 4
• *14*: Node number 14

Young's modulus $E = 2.77 \times 10^4$ psi
Poisson's ratio $\nu = 0.17$
Compressive strength $\sigma_{u,c} = 26.5$ psi
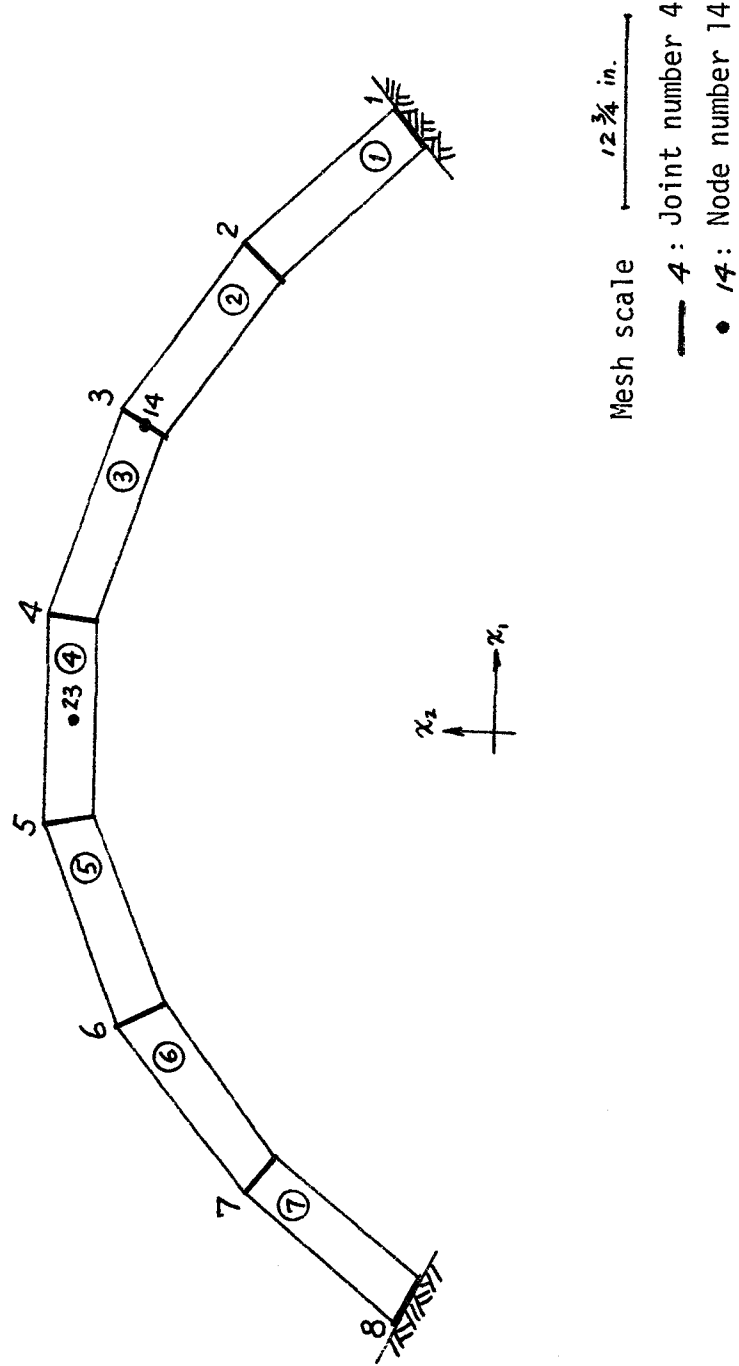Elastic-Perfect-Plastic Mat'l Model
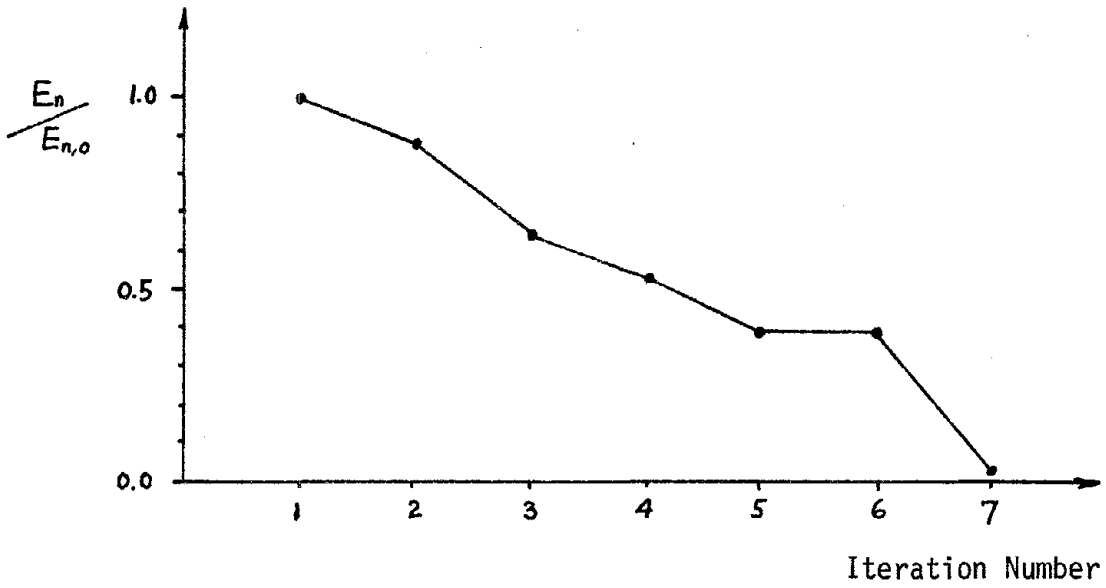Mat'l nonlinearity only at active joints

FIG. II-11 ARCH RIB BLOCKS AND JOINTS

(a)

Iteration Number
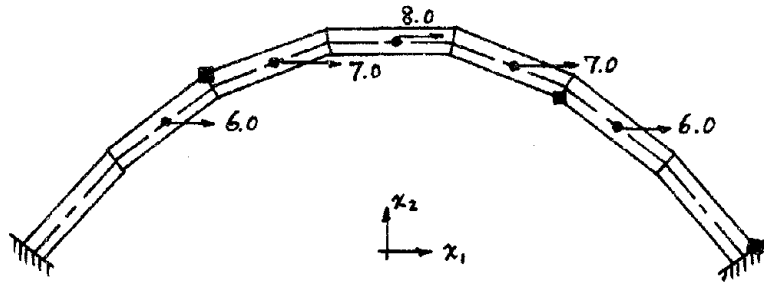
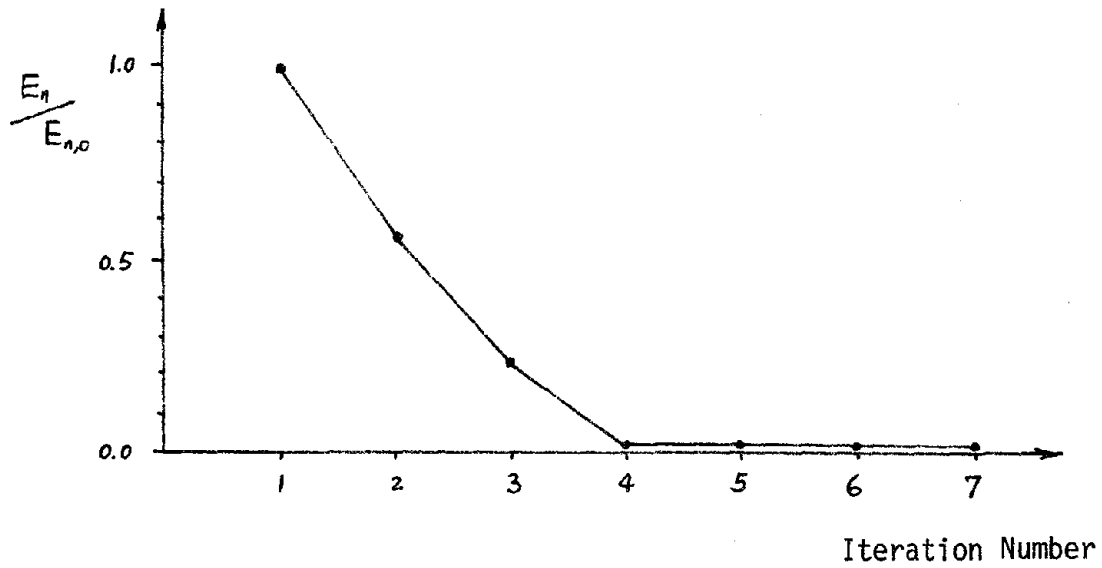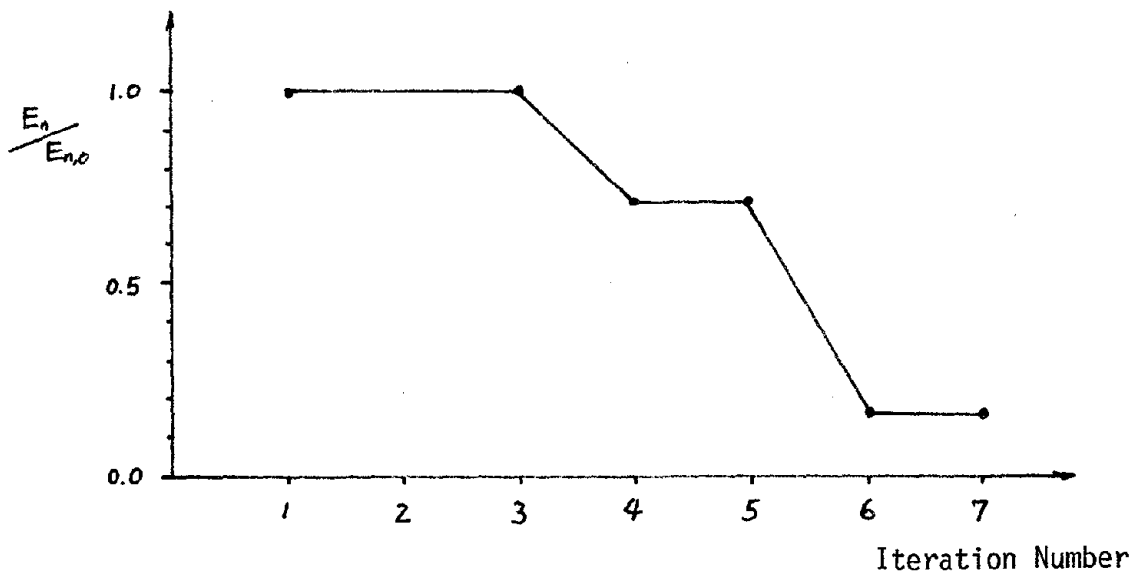(b) EXTRADOS OF JOINT-6

FIG. II-12 COMPRESSION FAILURE MECHANISM OF ARCH RIB

(c) EXTRADOS OF JOINT-1

(d) INTRADOS OF JOINT-3

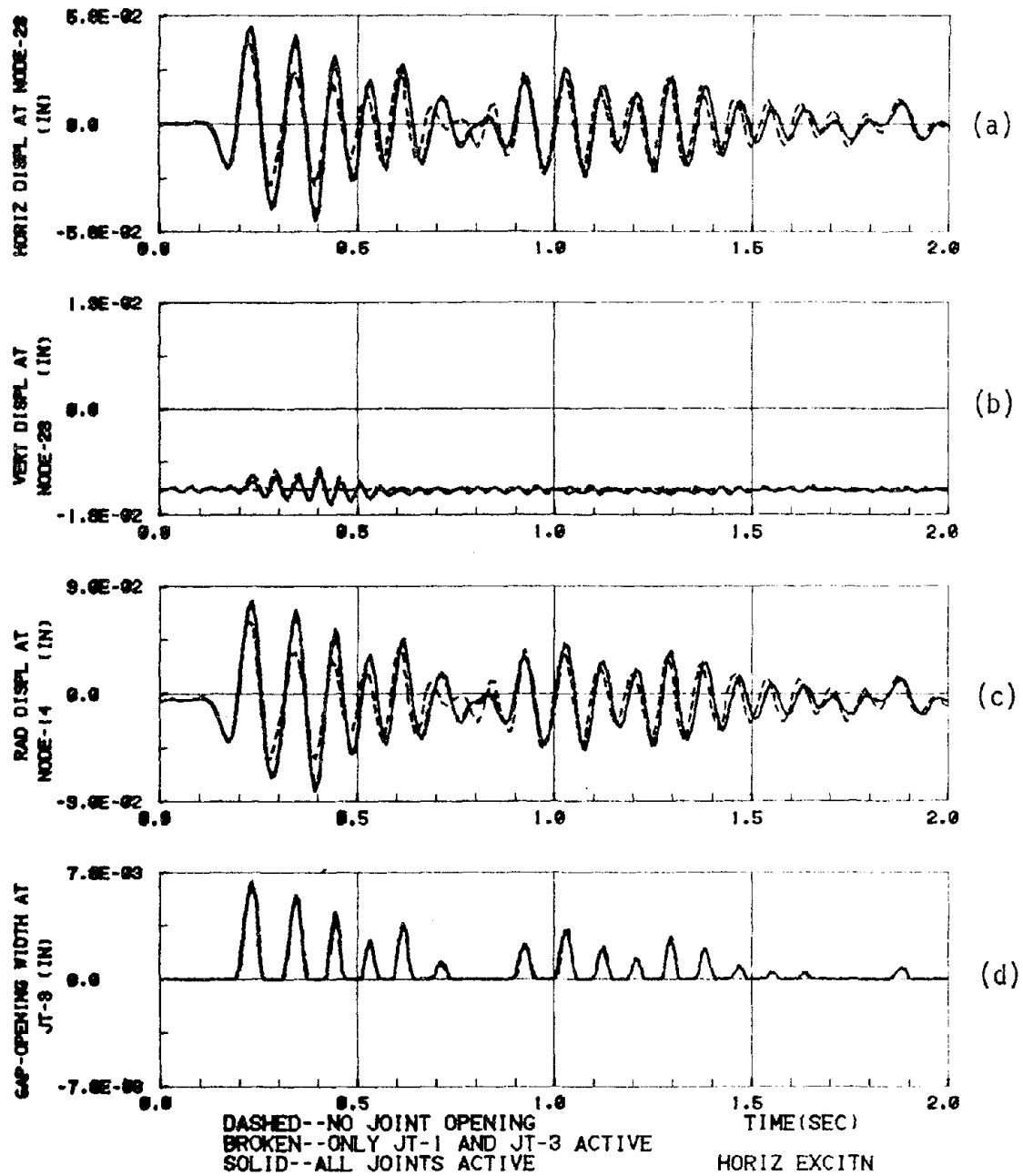FIG. II-12 (Cont.) COMPRESSION FAILURE MECHANISM OF ARCH RIB

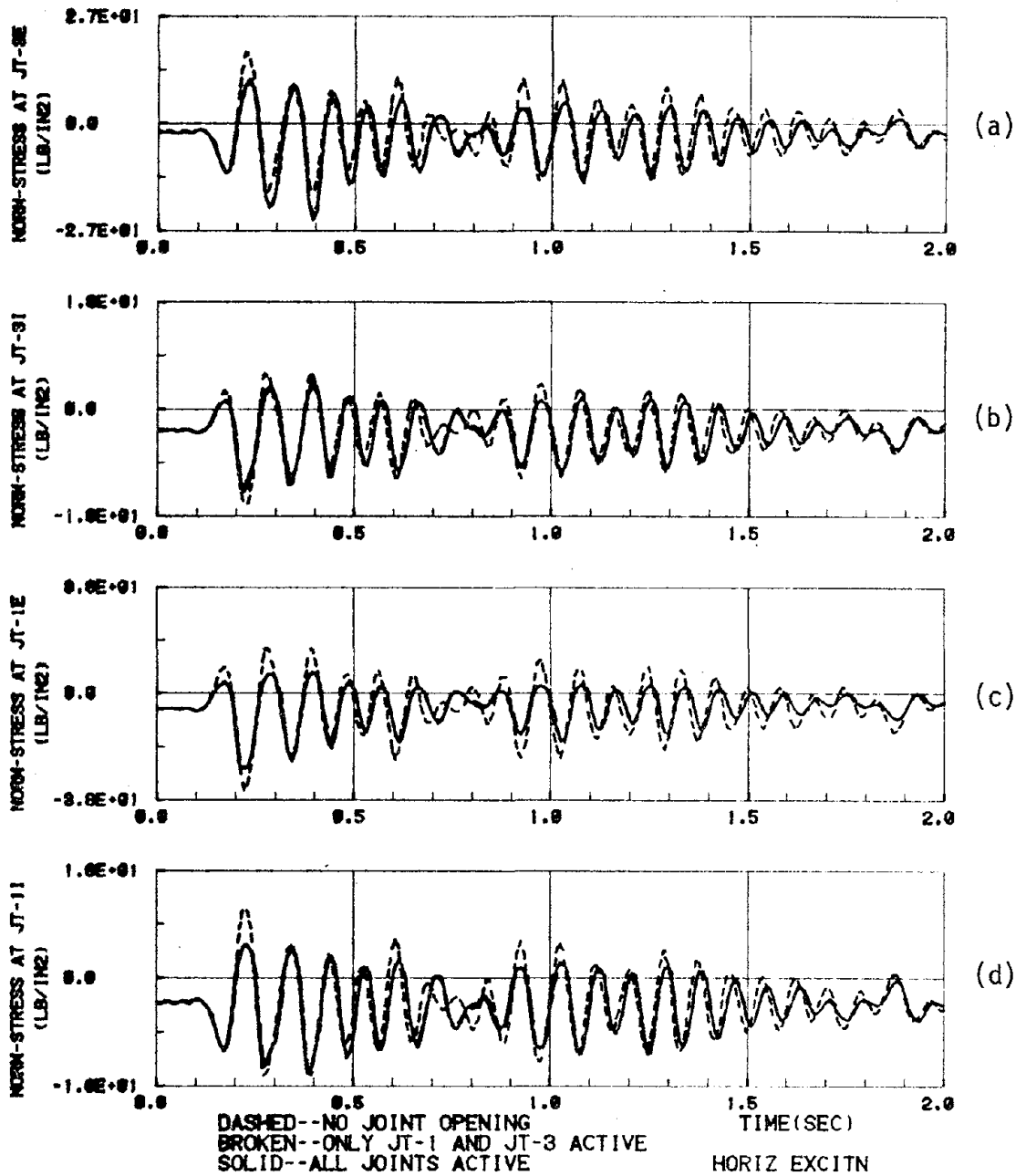FIG. II-13 DISPLACEMENT RESPONSE AND JOINT OPENING WIDTH
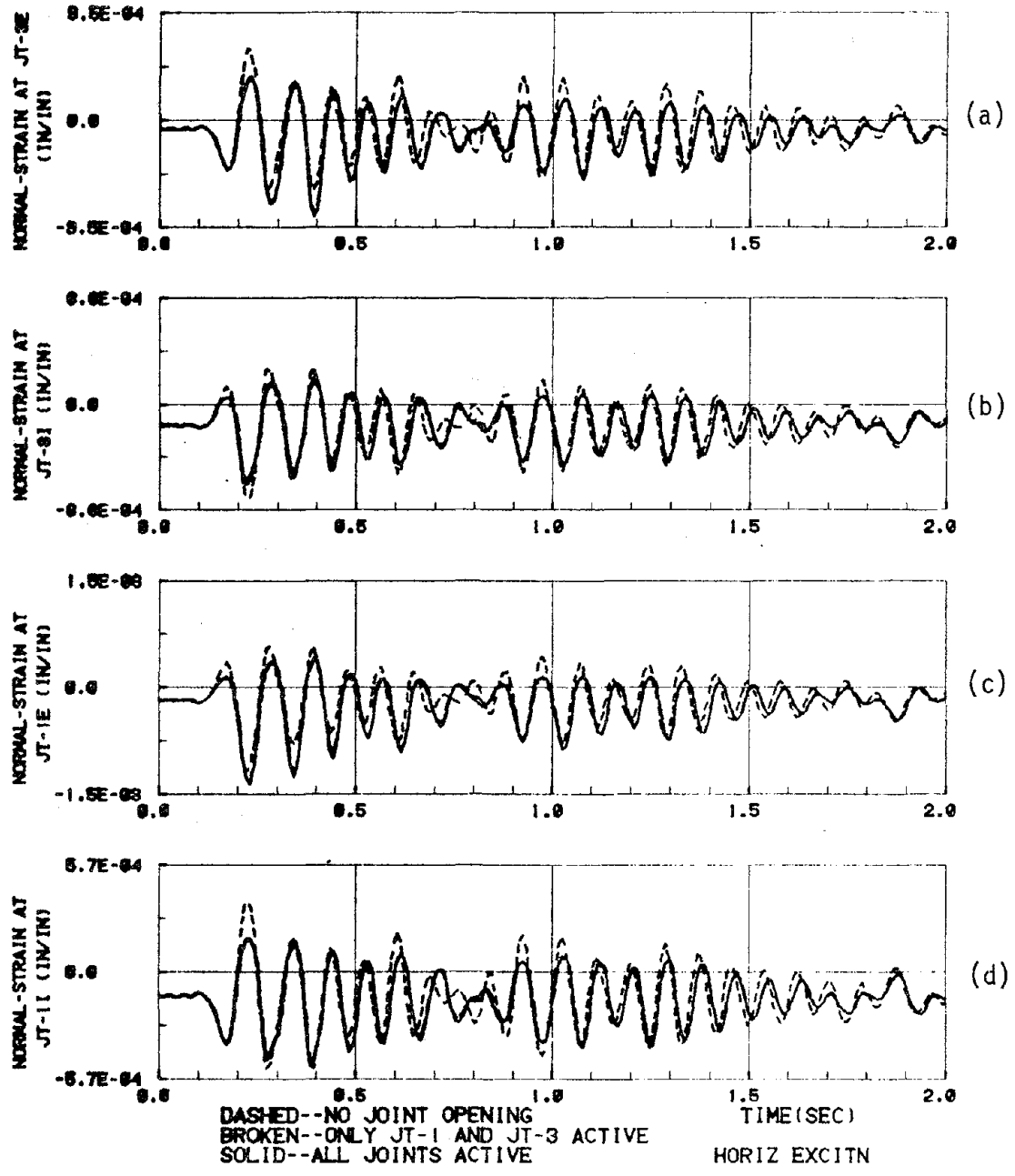
FIG. II-14 STRESS RESPONSE AT INTERFACE JOINTS

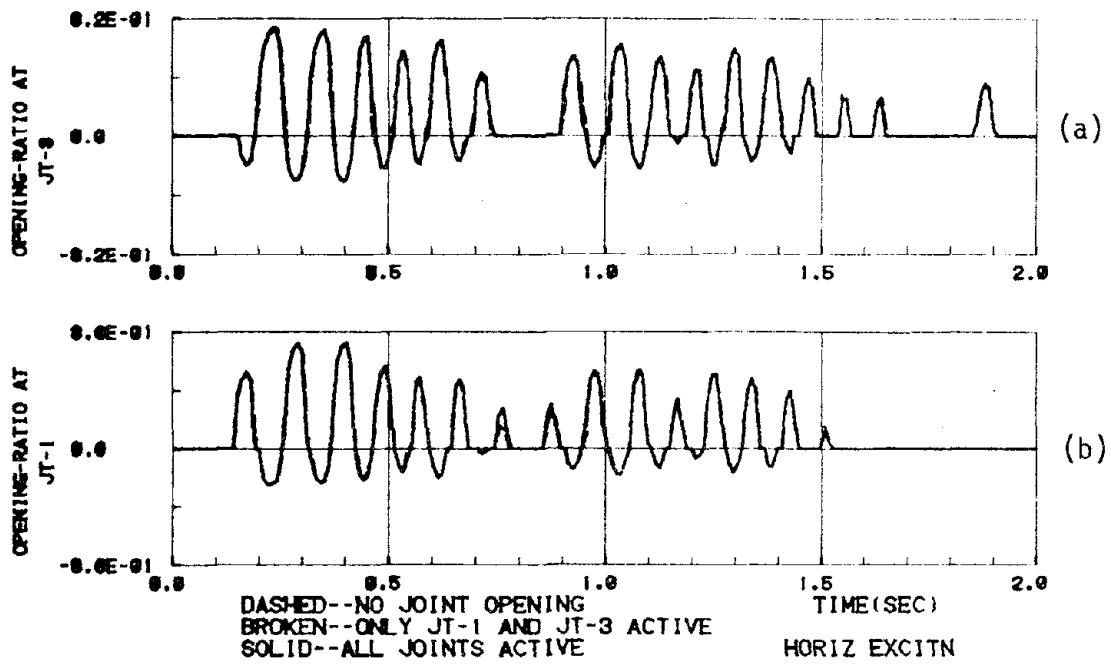FIG. II-15 STRAIN RESPONSE AT INTERFACE JOINTS

73

FIG. II-16 OPENING-RATIOS AT INTERFACE JOINTS

REFERENCES

(1)   Bergan, P. G. and Holand, I., "Nonlinear Finite Element Analysis of Concrete Structures", Computer Methods in Applied Mechanics and Engineering, 17/18(1979), pp. 443-467.

(2)   Aldstedt, E. and Bergan, P. G., "Nonlinear Time-Dependent Concrete-Frame Analysis", Journal of the Structural Division, ASCE, ST7, July 1978.

(3)   Sorensen, S. I., Arnesen, A. and Bergan, P. G., "Nonlinear Finite Element Analysis of Reinforced Concrete Using Endochronic Theory," in Finite Elements in Nonlinear Mechanics, Ed. J. T. Oden, International Conference at Geilo, Norway, Aug. 1977, Vol. 1.

(4)   Arnesen, A., Sorensen, S. I. and Bergan, P. G., "Nonlinear Analysis of Reinforced Concrete", International Conference on Engineering Application of the Finite Element Method, Hovik, Norway, May 9-11, 1979, Vol. 2.

(5)   Wilson, E. L., "Finite Elements for Foundations, Joints and Fluids," in Finite Elements in Geomechanics, Ed. G. Gudehus, John Wiley and Sons, Ltd., 1977.

(6)   Bazant, Z. P. and Tsubaki, T., "Slip-Dilatancy Model for Cracked Reinforced Concrete," Journal of the Structural Division, ASCE, ST9, Sept. 1980.

(7)   Goodman, R. E., Taylor, R. L. and Brekke, T. L., "A Model for the Mechanics of Jointed Rock", Journal of the Soil Mechanics and Foundation Division, Proceedings of ASCE, SM3, May 1968.

(8)   Clough, R. W., "Concrete Dams: Influence of Response Nonlinearities", Lecture Notes, June 1980.

(9)   Ghaboussi, J., Wilson, E. L. and Isenberg, J., "Finite Element for Rock Joints and Interfaces," Journal of the Soil Mechanics and Foundation Division, ASCE, SM10, Oct. 1973.

(10)   Chen, E. Y.-T. and Schnobrich, W. C., "Models for the Post-Cracking Behavior of Plain Concrete Under Short Term Monotonic Loading", Computers and Structures, Vol. 13, pp. 213-221, 1981.

(11)   Becker, J. M., Mueller, P. and Llorente, C., "Nonlinear Dynamic Analysis of Precast Concrete Walls", International Symposium for the Nonlinear Design of Concrete Structures, University of Waterloo, Canada, Aug. 7-9, 1979.

(12)   Petersson, H., "Application of the Finite Element Method in the Analysis of Contact Problems," in Finite Elements in Nonlinear Mechanics, Ed. J. T. Oden, International Conference at Geilo, Norway, Aug. 1977, Vol. 2.

(13) Hughes, T. J. R., Taylor, R. L., Sackman, J. L., Curnier, A. and Kanoknukulchai, W., "A Finite Element Method for a Class of Contact-Impact Problems", Computer Methods in Applied Mechanics and Engineering, 8(1976), pp. 249-276.

(14) Hughes, T. J. R., Taylor, R. L. and Kanoknukulchai, W., "A Finite Element Method for Large Displacement Contact and Impact Problems", Proceedings US-German Finite Element Symposium, MIT, Aug. 1976.

(15) Francavilla, A. and Zienkiewicz, O. C., "A Note on Numerical Computation of Elastic Contact Problems", International Journal for Numerical Methods in Engineering, Vol. 9, pp. 913-924, 1975.

(16) Taylor, R. L. and Sackman, J. L., "Contact-Impact Problems", Report No. SESM 78-4, Department of Civil Engineering, University of California, Berkeley, Dec. 1978.

(17) Pal, N., "Nonlinear Earthquake Response of Concrete Gravity Dams", Earthquake Engineering Research Center, Report No. EERC-74-14, Dec. 1974.

(18) Tseng, J. and Olson, M. D., "The Mixed Finite Element Method Applied to Two-Dimensional Elastic Contact Problems", International Journal for Numerical Methods in Engineering, Vol. 17, pp. 991-1014, 1981.

(19) Stadter, J. T. and Weiss, R. O., "Analysis of Contact Through Finite Element Gaps", Computers and Structures, Vol. 10, pp. 867-873, 1979.

(20) Hung, N. D. and de Saxce, G., "Frictionless Contact of Elastic Bodies by Finite Element Method and Mathematical Programming Technique", Computers and Structures, Vol. 11, pp. 55-67, 1980.

(21) Herrmann, L. R., "Finite Element Analysis of Contact Problems", Journal of the Engineering Mechanics Division, ASCE, EM5, Oct. 1978.

(22) Scordelis, A. C., "Finite Element Analysis of Reinforced Concrete Structures", Proceedings of the Speciality Conference on the Finite Element Method in Civil Engineering, Montreal, Canada, June 1-2, 1972.

(23) Bazant, Z. P. and Gambarova, P., "Rough Cracks in Reinforced Concrete", Journal of the Structural Division, ASCE, ST4, April 1980.

(24) Chen, W. F. and Ting, E. C., "Constitutive Models for Concrete Structures", Journal of the Engineering Mechanics Division, ASCE, EM1, Feb. 1980.

(25) Blaauwendraad, J. and Grootenboer, H. J., "Essentials for Discrete Crack Analysis", Advanced Mechanics of Reinforced Concrete, IABSE Colloquium, Delft, The Netherlands, pp. 442a-442j, 1981.

(26) Oden, J. T. and Branchli, H. J., "On the Calculation of Consistent Stress Distributions in Finite Element Approximations", International Journal for Numerical Methods in Engineering, Vol. 3, pp. 317-325, 1971.

(27) "State of the Art Report on Finite Element Analysis of Reinforced Concrete," ASCE Committee on Concrete and Masonry Structure, Preprint, Oct. 1980. Also Its References.

(28) Zienkiewicz, O. C., "The Finite Element Method", 3rd Ed., McGraw-Hill, 1977.

(29) Gallagher, R. H., "Finite Element Analysis, Fundamentals", Prentice Hall, 1975.

(30) Niwa, A. and Clough, R. W., "Shaking Table Research on Concrete Dam Models," Earthquake Engineering Research Center, Report No. UCB/EERC-80/05, University of California, Berkeley, Sept. 1980.

(31) Hittinger, M. and Goodman, R. E., "JTROCK-A Computer Program for Stress Analysis of Two-Dimensional, Discontinuous Rock Masses", Report No. UCB/GT/78-04, Department of Civil Engineering, University of California, Berkeley.

(32) Darwin, D. and Pecknold, D. A., "Nonlinear Biaxial Stress-Strain Law for Concrete", Journal of the Engineering Mechanics Division, Proceedings of ASCE, No. EM2, April 1977.

(33) Darwin, D. and Pecknold, D. A., "Analysis of RC Shear Panels Under Cyclic Loading", Journal of the Structural Division, Proceedings of ASCE, No. ST2, Feb. 1976.

(34) Taylor, R. L., "FEAP-Finite Element Analysis Program," Element ELMT12, SESM, Division of Civil Engineering, University of California, Berkeley, 1980.

(35) Clough, R. W. and Penzien, J., "Dynamics of Structures", McGraw-Hill, Inc., 1975.

(36) "Criteria and Assumptions for Numerical Analysis of Dams", Ed. D. J. Naylor, K. G. Stagg and O. C. Zienkiewicz, Proceedings of an International Symposium held at Swansea, United Kingdom, Sept. 8-11, 1975.

(37) Kuo, J. S.-H. and Clough, R. W., "NDARCH-A Program for Nonlinear Dynamic Analysis of Arch Ribs," EERC Report to appear, University of California, Berkeley.

(38) Bathe, K. J. and Wilson, E. L., "Numerical Methods in Finite Element Analysis", Prentice-Hall, Inc., 1976.

(39) Bathe, K. J., Wilson, E. L. and IDing, R. H., "NONSAP-A Structural Analysis Program for Static and Dynamic Response of Nonlinear Systems", Report No. UC SESM 74-3, Department of Civil Engineering, University of California, Berkeley, 1974.

(40) Priscu, R., Stematiu, D., Ilie, L. and Popovici, A., "Critical Considerations on Arch Dam Mathematical Models", pp. 263-284 of Reference (36).

(41) Holand, I., Rollen, A. and Aldstedt, E., "Nonlinear Analysis of Arch Dams", pp. 409-433 of Reference (36).

(42) Croucamp, W. S. and Grobbelaar, C., "The Three Dimensional Evaluation of the Effects of Structural Discontinuities in an Arch Dam and a Multiple Dome Dam", pp. 1033-1049 of Reference (36).

(43) Ricketts, R. E. and Zienkiewicz, O. C., "Preformed Cracks and Their Influence on Behavior of Concrete Dams", pp. 1127-1148 of Reference (36).

EARTHQUAKE ENGINEERING RESEARCH CENTER REPORTS

NOTE: Numbers in parentheses are Accession Numbers assigned by the National Technical Information Service; these are followed by a price code. Copies of the reports may be ordered from the National Technical Information Service, 5285 Port Royal Road, Springfield, Virginia, 22161. Accession Numbers should be quoted on orders for reports (PB --- ---) and remittance must accompany each order. Reports without this information were not available at time of printing. The complete list of EERC reports (from EERC 67-1) is available upon request from the Earthquake Engineering Research Center, University of California, Berkeley, 47th Street and Hoffman Boulevard, Richmond, California 94804.

UCB/EERC-77/01 "PLUSH - A Computer Program for Probabilistic Finite Element Analysis of Seismic Soil-Structure Interaction," by M.P. Romo Organista, J. Lysmer and H.B. Seed - 1977 (PB81 177 651)A05

UCB/EERC-77/02 "Soil-Structure Interaction Effects at the Humboldt Bay Power Plant in the Ferndale Earthquake of June 7, 1975," by J.E. Valera, H.B. Seed, C.F. Tsai and J. Lysmer - 1977 (PB 265 795)A04

UCB/EERC-77/03 "Influence of Sample Disturbance on Sand Response to Cyclic Loading," by K. Mori, H.B. Seed and C.K. Chan - 1977 (PB 267 352)A04

UCB/EERC-77/04 "Seismological Studies of Strong Motion Records," by J. Shoja-Taheri - 1977 (PB 269 655)A10

UCB/EERC-77/05 Unassigned

UCB/EERC-77/06 "Developing Methodologies for Evaluating the Earthquake Safety of Existing Buildings," by No. 1 - B. Bresler; No. 2 - B. Bresler, T. Okada and D. Zisling; No. 3 - T. Okada and B. Bresler; No. 4 - V.V. Bertero and B. Bresler - 1977 (PB 267 354)A08

UCB/EERC-77/07 "A Literature Survey - Transverse Strength of Masonry Walls," by Y. Omote, R.L. Mayes, S.W. Chen and R.W. Clough - 1977 (PB 277 933)A07

UCB/EERC-77/08 "DRAIN-TABS: A Computer Program for Inelastic Earthquake Response of Three Dimensional Buildings," by R. Guendelman-Israel and G.H. Powell - 1977 (PB 270 693)A07

UCB/EERC-77/09 "SUBWALL: A Special Purpose Finite Element Computer Program for Practical Elastic Analysis and Design of Structural Walls with Substructure Option," by D.Q. Le, H. Peterson and E.P. Popov - 1977 (PB 270 567)A05

UCB/EERC-77/10 "Experimental Evaluation of Seismic Design Methods for Broad Cylindrical Tanks," by D.P. Clough (PB 272 280)A13

UCB/EERC-77/11 "Earthquake Engineering Research at Berkeley - 1976," - 1977 (PB 273 507)A09

UCB/EERC-77/12 "Automated Design of Earthquake Resistant Multistory Steel Building Frames," by N.D. Walker, Jr. - 1977 (PB 276 526)A09

UCB/EERC-77/13 "Concrete Confined by Rectangular Hoops Subjected to Axial Loads," by J. Vallenas, V.V. Bertero and E.P. Popov - 1977 (PB 275 165)A06

UCB/EERC-77/14 "Seismic Strain Induced in the Ground During Earthquakes," by Y. Sugimura - 1977 (PB 284 201)A04

UCB/EERC-77/15 Unassigned

UCB/EERC-77/16 "Computer Aided Optimum Design of Ductile Reinforced Concrete Moment Resisting Frames," by S.W. Zagajeski and V.V. Bertero - 1977 (PB 280 137)A07

UCB/EERC-77/17 "Earthquake Simulation Testing of a Stepping Frame with Energy-Absorbing Devices," by J.M. Kelly and D.F. Tsztoo - 1977 (PB 273 506)A04

UCB/EERC-77/18 "Inelastic Behavior of Eccentrically Braced Steel Frames under Cyclic Loadings," by C.W. Roeder and E.P. Popov - 1977 (PB 275 526)A15

UCB/EERC-77/19 "A Simplified Procedure for Estimating Earthquake-Induced Deformations in Dams and Embankments," by F.I. Makdisi and H.B. Seed - 1977 (PB 276 820)A04

UCB/EERC-77/20 "The Performance of Earth Dams during Earthquakes," by H.B. Seed, F.I. Makdisi and P. de Alba - 1977 (PB 276 821)A04

UCB/EERC-77/21 "Dynamic Plastic Analysis Using Stress Resultant Finite Element Formulation," by P. Lukkunapvasit and J.M. Kelly - 1977 (PB 275 453)A04

UCB/EERC-77/22 "Preliminary Experimental Study of Seismic Uplift of a Steel Frame," by R.W. Clough and A.A. Huckelbridge 1977 (PB 278 769)A08

UCB/EERC-77/23 "Earthquake Simulator Tests of a Nine-Story Steel Frame with Columns Allowed to Uplift," by A.A. Huckelbridge - 1977 (PB 277 944)A09

UCB/EERC-77/24 "Nonlinear Soil-Structure Interaction of Skew Highway Bridges," by M.-C. Chen and J. Penzien - 1977 (PB 276 176)A07

UCB/EERC-77/25 "Seismic Analysis of an Offshore Structure Supported on Pile Foundations," by D.D.-N. Liou and J. Penzien 1977 (PB 283 180)A06

UCB/EERC-77/26 "Dynamic Stiffness Matrices for Homogeneous Viscoelastic Half-Planes," by G. Dasgupta and A.K. Chopra - 1977 (PB 279 654)A06

Preceding page blank

UCB/EERC-77/27   "A Practical Soft Story Earthquake Isolation System," by J.M. Kelly, J.M. Eidinger and C.J. Derham - 1977 (PB 276 814)A07

UCB/EERC-77/28   "Seismic Safety of Existing Buildings and Incentives for Hazard Mitigation in San Francisco: An Exploratory Study," by A.J. Meltsner - 1977 (PB 281 970)A05

UCB/EERC-77/29   "Dynamic Analysis of Electrohydraulic Shaking Tables," by D. Rea, S. Abedi-Hayati and Y. Takahashi 1977 (PB 282 569)A04

UCB/EERC-77/30   "An Approach for Improving Seismic - Resistant Behavior of Reinforced Concrete Interior Joints," by B. Galunic, V.V. Bertero and E.P. Popov - 1977 (PB 290 870)A06

UCB/EERC-78/01   "The Development of Energy-Absorbing Devices for Aseismic Base Isolation Systems," by J.M. Kelly and D.F. Tsztoo - 1978 (PB 284 978)A04

UCB/EERC-78/02   "Effect of Tensile Prestrain on the Cyclic Response of Structural Steel Connections, by J.G. Bouwkamp and A. Mukhopadhyay - 1978

UCB/EERC-78/03   "Experimental Results of an Earthquake Isolation System using Natural Rubber Bearings," by J.M. Eidinger and J.M. Kelly - 1978 (PB 281 686)A04

UCB/EERC-78/04   "Seismic Behavior of Tall Liquid Storage Tanks," by A. Niwa - 1978 (PB 284 017)A14

UCB/EERC-78/05   "Hysteretic Behavior of Reinforced Concrete Columns Subjected to High Axial and Cyclic Shear Forces," by S.W. Zagajeski, V.V. Bertero and J.G. Bouwkamp - 1978 (PB 283 858)A13

UCB/EERC-78/06   "Three Dimensional Inelastic Frame Elements for the ANSR-I Program," by A. Riahi, D.G. Row and G.H. Powell - 1978 (PB 295 755)A04

UCB/EERC-78/07   "Studies of Structural Response to Earthquake Ground Motion," by O.A. Lopez and A.K. Chopra - 1978 (PB 282 790)A05

UCB/EERC-78/08   "A Laboratory Study of the Fluid-Structure Interaction of Submerged Tanks and Caissons in Earthquakes," by R.C. Byrd - 1978 (PB 284 957)A08

UCB/EERC-78/09   Unassigned

UCB/EERC-78/10   "Seismic Performance of Nonstructural and Secondary Structural Elements," by I. Sakamoto - 1978 (PB81 154 593)A05

UCB/EERC-78/11   "Mathematical Modelling of Hysteresis Loops for Reinforced Concrete Columns," by S. Nakata, T. Sproul and J. Penzien - 1978 (PB 298 274)A05

UCB/EERC-78/12   "Damageability in Existing Buildings," by T. Blejwas and B. Bresler - 1978 (PB 80 166 978)A05

UCB/EERC-78/13   "Dynamic Behavior of a Pedestal Base Multistory Building," by R.M. Stephen, E.L. Wilson, J.G. Bouwkamp and M. Button - 1978 (PB 286 650)A08

UCB/EERC-78/14   "Seismic Response of Bridges - Case Studies," by R.A. Imbsen, V. Nutt and J. Penzien - 1978 (PB 286 503)A10

UCB/EERC-78/15   "A Substructure Technique for Nonlinear Static and Dynamic Analysis," by D.G. Row and G.H. Powell - 1978 (PB 288 077)A10

UCB/EERC-78/16   "Seismic Risk Studies for San Francisco and for the Greater San Francisco Bay Area," by C.S. Oliveira - 1978 (PB 81 120 115)A07

UCB/EERC-78/17   "Strength of Timber Roof Connections Subjected to Cyclic Loads," by P. Gülkan, R.L. Mayes and R.W. Clough - 1978 (HUD-000 1491)A07

UCB/EERC-78/18   "Response of K-Braced Steel Frame Models to Lateral Loads," by J.G. Bouwkamp, R.M. Stephen and E.P. Popov - 1978

UCB/EERC-78/19   "Rational Design Methods for Light Equipment in Structures Subjected to Ground Motion," by J.L. Sackman and J.M. Kelly - 1978 (PB 292 357)A04

UCB/EERC-78/20   "Testing of a Wind Restraint for Aseismic Base Isolation," by J.M. Kelly and D.E. Chitty - 1978 (PB 292 833)A03

UCB/EERC-78/21   "APOLLO - A Computer Program for the Analysis of Pore Pressure Generation and Dissipation in Horizontal Sand Layers During Cyclic or Earthquake Loading," by P.P. Martin and H.B. Seed - 1978 (PB 292 835)A04

UCB/EERC-78/22   "Optimal Design of an Earthquake Isolation System," by M.A. Bhatti, K.S. Pister and E. Polak - 1978 (PB 294 735)A06

UCB/EERC-78/23   "MASH - A Computer Program for the Non-Linear Analysis of Vertically Propagating Shear Waves in Horizontally Layered Deposits," by P.P. Martin and H.B. Seed - 1978 (PB 293 101)A05

UCB/EERC-78/24   "Investigation of the Elastic Characteristics of a Three Story Steel Frame Using System Identification," by I. Kaya and H.D. McNiven - 1978 (PB 296 225)A06

UCB/EERC-78/25   "Investigation of the Nonlinear Characteristics of a Three-Story Steel Frame Using System Identification," by I. Kaya and H.D. McNiven - 1978 (PB 301 363)A05

UCB/EERC-78/26 "Studies of Strong Ground Motion in Taiwan," by Y.M. Hsiung, B.A. Bolt and J. Penzien - 1978 (PB 298 436)A06

UCB/EERC-78/27 "Cyclic Loading Tests of Masonry Single Piers: Volume 1 - Height to Width Ratio of 2," by P.A. Hidalgo, R.L. Mayes, H.D. McNiven and R.W. Clough - 1978 (PB 296 211)A07

UCB/EERC-78/28 "Cyclic Loading Tests of Masonry Single Piers: Volume 2 - Height to Width Ratio of 1," by S.-W.J. Chen, P.A. Hidalgo, R.L. Mayes, R.W. Clough and H.D. McNiven - 1978 (PB 296 212)A09

UCB/EERC-78/29 "Analytical Procedures in Soil Dynamics," by J. Lysmer - 1978 (PB 298 445)A06

UCB/EERC-79/01 "Hysteretic Behavior of Lightweight Reinforced Concrete Beam-Column Subassemblages," by B. Forzani, E.P. Popov and V.V. Bertero - April 1979(PB 298 267)A06

UCB/EERC-79/02 "The Development of a Mathematical Model to Predict the Flexural Response of Reinforced Concrete Beams to Cyclic Loads, Using System Identification," by J. Stanton & H. McNiven - Jan. 1979(PB 295 875)A10

UCB/EERC-79/03 "Linear and Nonlinear Earthquake Response of Simple Torsionally Coupled Systems," by C.L. Kan and A.K. Chopra - Feb. 1979(PB 298 262)A06

UCB/EERC-79/04 "A Mathematical Model of Masonry for Predicting its Linear Seismic Response Characteristics," by Y. Mengi and H.D. McNiven - Feb. 1979(PB 298 266)A06

UCB/EERC-79/05 "Mechanical Behavior of Lightweight Concrete Confined by Different Types of Lateral Reinforcement," by M.A. Manrique, V.V. Bertero and E.P. Popov - May 1979(PB 301 114)A06

UCB/EERC-79/06 "Static Tilt Tests of a Tall Cylindrical Liquid Storage Tank," by R.W. Clough and A. Niwa - Feb. 1979 (PB 301 167)A06

UCB/EERC-79/07 "The Design of Steel Energy Absorbing Restrainers and Their Incorporation into Nuclear Power Plants for Enhanced Safety: Volume 1 - Summary Report," by P.N. Spencer, V.F. Zackay, and E.R. Parker - Feb. 1979(UCB/EERC-79/07)A09

UCB/EERC-79/08 "The Design of Steel Energy Absorbing Restrainers and Their Incorporation into Nuclear Power Plants for Enhanced Safety: Volume 2 - The Development of Analyses for Reactor System Piping,""Simple Systems" by M.C. Lee, J. Penzien, A.K. Chopra and K, Suzuki "Complex Systems" by G.H. Powell, E.L. Wilson, R.W. Clough and D.G. Row - Feb. 1979(UCB/EERC-79/08)A10

UCB/EERC-79/09 "The Design of Steel Energy Absorbing Restrainers and Their Incorporation into Nuclear Power Plants for Enhanced Safety: Volume 3 - Evaluation of Commercial Steels," by W.S. Owen, R.M.N. Pelloux, R.O. Ritchie, M. Faral, T. Ohhashi, J. Toplosky, S.J. Hartman, V.F. Zackay and E.R. Parker - Feb. 1979(UCB/EERC-79/09)A04

UCB/EERC-79/10 "The Design of Steel Energy Absorbing Restrainers and Their Incorporation into Nuclear Power Plants for Enhanced Safety: Volume 4 - A Review of Energy-Absorbing Devices," by J.M. Kelly and M.S. Skinner - Feb. 1979(UCB/EERC-79/10)A04

UCB/EERC-79/11 "Conservatism In Summation Rules for Closely Spaced Modes," by J.M. Kelly and J.L. Sackman - May 1979(PB 301 328)A03

UCB/EERC-79/12 "Cyclic Loading Tests of Masonry Single Piers; Volume 3 - Height to Width Ratio of 0.5," by P.A. Hidalgo, R.L. Mayes, H.D. McNiven and R.W. Clough - May 1979(PB 301 321)A08

UCB/EERC-79/13 "Cyclic Behavior of Dense Course-Grained Materials in Relation to the Seismic Stability of Dams," by N.G. Banerjee, H.B. Seed and C.K. Chan - June 1979(PB 301 373)A13

UCB/EERC-79/14 "Seismic Behavior of Reinforced Concrete Interior Beam-Column Subassemblages," by S. Viwathanatepa, E.P. Popov and V.V. Bertero - June 1979(PB 301 326)A10

UCB/EERC-79/15 "Optimal Design of Localized Nonlinear Systems with Dual Performance Criteria Under Earthquake Excitations," by M.A. Bhatti - July 1979(PB 80 167 109)A06

UCB/EERC-79/16 "OPTDYN - A General Purpose Optimization Program for Problems with or without Dynamic Constraints," by M.A. Bhatti, E. Polak and K.S. Pister - July 1979(PB 80 167 091)A05

UCB/EERC-79/17 "ANSR-II, Analysis of Nonlinear Structural Response, Users Manual," by D.P. Mondkar and G.H. Powell July 1979(PB 80 113 301)A05

UCB/EERC-79/18 "Soil Structure Interaction in Different Seismic Environments," A. Gomez-Masso, J. Lysmer, J.-C. Chen and H.B. Seed - August 1979(PB 80 101 520)A04

UCB/EERC-79/19 "ARMA Models for Earthquake Ground Motions," by M.K. Chang, J.W. Kwiatkowski, R.F. Nau, R.M. Oliver and K.S. Pister - July 1979(PB 301 166)A05

UCB/EERC-79/20 "Hysteretic Behavior of Reinforced Concrete Structural Walls," by J.M. Vallenas, V.V. Bertero and E.P. Popov - August 1979(PB 80 165 905)A12

UCB/EERC-79/21 "Studies on High-Frequency Vibrations of Buildings - 1: The Column Effect," by J. Lubliner - August 1979 (PB 80 158 553)A03

UCB/EERC-79/22 "Effects of Generalized Loadings on Bond Reinforcing Bars Embedded in Confined Concrete Blocks," by S. Viwathanatepa, E.P. Popov and V.V. Bertero - August 1979(PB 81 124 018)A14

UCB/EERC-79/23 "Shaking Table Study of Single-Story Masonry Houses, Volume 1: Test Structures 1 and 2," by P. Gülkan, R.L. Mayes and R.W. Clough - Sept. 1979 (HUD-000 1763)A12

UCB/EERC-79/24 "Shaking Table Study of Single-Story Masonry Houses, Volume 2: Test Structures 3 and 4," by P. Gülkan, R.L. Mayes and R.W. Clough - Sept. 1979 (HUD-000 1836)A12

UCB/EERC-79/25 "Shaking Table Study of Single-Story Masonry Houses, Volume 3: Summary, Conclusions and Recommendations," by R.W. Clough, R.L. Mayes and P. Gülkan - Sept. 1979 (HUD-000 1837)A06

UCB/EERC-79/26   "Recommendations for a U.S.-Japan Cooperative Research Program Utilizing Large-Scale Testing Facilities," by U.S.-Japan Planning Group - Sept. 1979(PB 301 407)A06

UCB/EERC-79/27   "Earthquake-Induced Liquefaction Near Lake Amatitlan, Guatemala," by H.B. Seed, I. Arango, C.K. Chan, A. Gomez-Masso and R. Grant de Ascoli - Sept. 1979(NUREG-CR1341)A03

UCB/EERC-79/28   "Infill Panels: Their Influence on Seismic Response of Buildings," by J.W. Axley and V.V. Bertero Sept. 1979(PB 80 163 371)A10

UCB/EERC-79/29   "3D Truss Bar Element (Type 1) for the ANSR-II Program," by D.P. Mondkar and G.H. Powell - Nov. 1979 (PB 80 169 709)A02

UCB/EERC-79/30   "2D Beam-Column Element (Type 5 - Parallel Element Theory) for the ANSR-II Program," by D.G. Row, G.H. Powell and D.P. Mondkar - Dec. 1979(PB 80 167 224)A03

UCB/EERC-79/31   "3D Beam-Column Element (Type 2 - Parallel Element Theory) for the ANSR-II Program," by A. Riahi, G.H. Powell and D.P. Mondkar - Dec. 1979(PB 80 167 216)A03

UCB/EERC-79/32   "On Response of Structures to Stationary Excitation," by A. Der Kiureghian - Dec. 1979(PB 80166 929)A03

UCB/EERC-79/33   "Undisturbed Sampling and Cyclic Load Testing of Sands," by S. Singh, H.B. Seed and C.K. Chan Dec. 1979(ADA 087 298)A07

UCB/EERC-79/34   "Interaction Effects of Simultaneous Torsional and Compressional Cyclic Loading of Sand," by P.M. Griffin and W.N. Houston - Dec. 1979(ADA 092 352)A15

UCB/EERC-80/01   "Earthquake Response of Concrete Gravity Dams Including Hydrodynamic and Foundation Interaction Effects," by A.K. Chopra, P. Chakrabarti and S. Gupta - Jan. 1980(AD-A087297)A10

UCB/EERC-80/02   "Rocking Response of Rigid Blocks to Earthquakes," by C.S. Yim, A.K. Chopra and J. Penzien - Jan. 1980 (PB80 166 002)A04

UCB/EERC-80/03   "Optimum Inelastic Design of Seismic-Resistant Reinforced Concrete Frame Structures," by S.W. Zagajeski and V.V. Bertero - Jan. 1980(PB80 164 635)A06

UCB/EERC-80/04   "Effects of Amount and Arrangement of Wall-Panel Reinforcement on Hysteretic Behavior of Reinforced Concrete Walls," by R. Iliya and V.V. Bertero - Feb. 1980(PB81 122 525)A09

UCB/EERC-80/05   "Shaking Table Research on Concrete Dam Models," by A. Niwa and R.W. Clough - Sept. 1980(PB81 122 368)A06

UCB/EERC-80/06   "The Design of Steel Energy-Absorbing Restrainers and their Incorporation into Nuclear Power Plants for Enhanced Safety (Vol 1A): Piping with Energy Absorbing Restrainers: Parameter Study on Small Systems," by G.H. Powell, C. Oughourlian and J. Simons - June 1980

UCB/EERC-80/07   "Inelastic Torsional Response of Structures Subjected to Earthquake Ground Motions," by Y. Yamazaki April 1980(PB81 122 327)A08

UCB/EERC-80/08   "Study of X-Braced Steel Frame Structures Under Earthquake Simulation," by Y. Ghanaat - April 1980 (PB81 122 335)A11

UCB/EERC-80/09   "Hybrid Modelling of Soil-Structure Interaction," by S. Gupta, T.W. Lin, J. Penzien and C.S. Yeh May 1980(PB81 122 319)A07

UCB/EERC-80/10   "General Applicability of a Nonlinear Model of a One Story Steel Frame," by B.I. Sveinsson and H.D. McNiven - May 1980(PB81 124 877)A06

UCB/EERC-80/11   "A Green-Function Method for Wave Interaction with a Submerged Body," by W. Kioka - April 1980 (PB81 122 269)A07

UCB/EERC-80/12   "Hydrodynamic Pressure and Added Mass for Axisymmetric Bodies," by F. Nilrat - May 1980(PB81 122 343)A08

UCB/EERC-80/13   "Treatment of Non-Linear Drag Forces Acting on Offshore Platforms," by B.V. Dao and J. Penzien May 1980(PB81 153 413)A07

UCB/EERC-80/14   "2D Plane/Axisymmetric Solid Element (Type 3 - Elastic or Elastic-Perfectly Plastic) for the ANSR-II Program," by D.P. Mondkar and G.H. Powell - July 1980(PB81 122 350)A03

UCB/EERC-80/15   "A Response Spectrum Method for Random Vibrations," by A. Der Kiureghian - June 1980(PB81 122 301)A03

UCB/EERC-80/16   "Cyclic Inelastic Buckling of Tubular Steel Braces," by V.A. Zayas, E.P. Popov and S.A. Mahin June 1980(PB81 124 885)A10

UCB/EERC-80/17   "Dynamic Response of Simple Arch Dams Including Hydrodynamic Interaction," by C.S. Porter and A.K. Chopra - July 1980(PB81 124 000)A13

UCB/EERC-80/18   "Experimental Testing of a Friction Damped Aseismic Base Isolation System with Fail-Safe Characteristics," by J.M. Kelly, K.E. Beucke and M.S. Skinner - July 1980(PB81 148 595)A04

UCB/EERC-80/19   "The Design of Steel Energy-Absorbing Restrainers and their Incorporation into Nuclear Power Plants for Enhanced Safety (Vol 1B): Stochastic Seismic Analyses of Nuclear Power Plant Structures and Piping Systems Subjected to Multiple Support Excitations," by M.C. Lee and J. Penzien - June 1980

UCB/EERC-80/20   "The Design of Steel Energy-Absorbing Restrainers and their Incorporation into Nuclear Power Plants for Enhanced Safety (Vol 1C): Numerical Method for Dynamic Substructure Analysis," by J.M. Dickens and E.L. Wilson - June 1980

UCB/EERC-80/21   "The Design of Steel Energy-Absorbing Restrainers and their Incorporation into Nuclear Power Plants for Enhanced Safety (Vol 2): Development and Testing of Restraints for Nuclear Piping Systems," by J.M. Kelly and M.S. Skinner - June 1980

UCB/EERC-80/22   "3D Solid Element (Type 4-Elastic or Elastic-Perfectly-Plastic) for the ANSR-II Program," by D.P. Mondkar and G.H. Powell - July 1980(PB81 123 242)A03

UCB/EERC-80/23   "Gap-Friction Element (Type 5) for the ANSR-II Program," by D.P. Mondkar and G.H. Powell - July 1980 (PB81 122 285)A03

UCB/EERC-80/24   "U-Bar Restraint Element (Type 11) for the ANSR-II Program," by C. Oughourlian and G.H. Powell
July 1980(PB81 122 293)A03

UCB/EERC-80/25   "Testing of a Natural Rubber Base Isolation System by an Explosively Simulated Earthquake," by
J.M. Kelly - August 1980(PB81 201 360)A04

UCB/EERC-80/26   "Input Identification from Structural Vibrational Response," by Y. Hu - August 1980(PB81 152 308)A05

UCB/EERC-80/27   "Cyclic Inelastic Behavior of Steel Offshore Structures," by V.A. Zayas, S.A. Mahin and E.P. Popov
August 1980(PB81 196 180)A15

UCB/EERC-80/28   "Shaking Table Testing of a Reinforced Concrete Frame with Biaxial Response," by M.G. Oliva
October 1980(PB81 154 304)A10

UCB/EERC-80/29   "Dynamic Properties of a Twelve-Story Prefabricated Panel Building," by J.G. Bouwkamp, J.P. Kollegger
and R.M. Stephen - October 1980(PB82 117 128)A06

UCB/EERC-80/30   "Dynamic Properties of an Eight-Story Prefabricated Panel Building," by J.G. Bouwkamp, J.P. Kollegger
and R.M. Stephen - October 1980(PB81 200 313)A05

UCB/EERC-80/31   "Predictive Dynamic Response of Panel Type Structures Under Earthquakes," by J.P. Kollegger and
J.G. Bouwkamp - October 1980(PB81 152 316)A04

UCB/EERC-80/32   "The Design of Steel Energy-Absorbing Restrainers and their Incorporation into Nuclear Power Plants
for Enhanced Safety (Vol 3): Testing of Commercial Steels in Low-Cycle Torsional Fatigue," by
P. Spencer, E.R. Parker, E. Jongewaard and M. Drory

UCB/EERC-80/33   "The Design of Steel Energy-Absorbing Restrainers and their Incorporation into Nuclear Power Plants
for Enhanced Safety (Vol 4): Shaking Table Tests of Piping Systems with Energy-Absorbing Restrainers,"
by S.F. Stiemer and W.G. Godden - Sept. 1980

UCB/EERC-80/34   "The Design of Steel Energy-Absorbing Restrainers and their Incorporation into Nuclear Power Plants
for Enhanced Safety (Vol 5): Summary Report," by P. Spencer

UCB/EERC-80/35   "Experimental Testing of an Energy-Absorbing Base Isolation System," by J.M. Kelly, M.S. Skinner and
K.E. Beucke - October 1980(PB81 154 072)A04

UCB/EERC-80/36   "Simulating and Analyzing Artificial Non-Stationary Earthquake Ground Motions," by R.F. Nau, R.M. Oliver
and K.S. Pister - October 1980(PB81 153 397)A04

UCB/EERC-80/37   "Earthquake Engineering at Berkeley - 1980," - Sept. 1980(PB81 205 874)A09

UCB/EERC-80/38   "Inelastic Seismic Analysis of Large Panel Buildings," by V. Schricker and G.H. Powell - Sept. 1980
(PB81 154 338)A13

UCB/EERC-80/39   "Dynamic Response of Embankment, Concrete-Gravity and Arch Dams Including Hydrodynamic Interaction,"
by J.F. Hall and A.K. Chopra - October 1980(PB81 152 324)A11

UCB/EERC-80/40   "Inelastic Buckling of Steel Struts Under Cyclic Load Reversal," by R.G. Black, W.A. Wenger and
E.P. Popov - October 1980(PB81 154 312)A08

UCB/EERC-80/41   "Influence of Site Characteristics on Building Damage During the October 3, 1974 Lima Earthquake," by
P. Repetto, I. Arango and H.B. Seed - Sept. 1980(PB81 161 739)A05

UCB/EERC-80/42   "Evaluation of a Shaking Table Test Program on Response Behavior of a Two Story Reinforced Concrete
Frame," by J.M. Blondet, R.W. Clough and S.A. Mahin

UCB/EERC-80/43   "Modelling of Soil-Structure Interaction by Finite and Infinite Elements," by F. Medina -
December 1980(PB81 229 270)A04

UCB/EERC-81/01   "Control of Seismic Response of Piping Systems and Other Structures by Base Isolation," edited by J.M.
Kelly - January 1981 (PB81 200 735)A05

UCB/EERC-81/02   "OPTNSR - An Interactive Software System for Optimal Design of Statically and Dynamically Loaded
Structures with Nonlinear Response," by M.A. Bhatti, V. Ciampi and K.S. Pister - January 1981
(PB81 218 851)A09

UCB/EERC-81/03   "Analysis of Local Variations in Free Field Seismic Ground Motions," by J.-C. Chen, J. Lysmer and H.B.
Seed - January 1981 (AD-A099508)A13

UCB/EERC-81/04   "Inelastic Structural Modeling of Braced Offshore Platforms for Seismic Loading," by V.A. Zayas,
P.-S.B. Shing, S.A. Mahin and E.P. Popov - January 1981(PB82 138 777)A07

UCB/EERC-81/05   "Dynamic Response of Light Equipment in Structures," by A. Der Kiureghian, J.L. Sackman and B. Nour-
Omid - April 1981 (PB81 218 497)A04

UCB/EERC-81/06   "Preliminary Experimental Investigation of a Broad Base Liquid Storage Tank," by J.G. Bouwkamp, J.P.
Kollegger and R.M. Stephen - May 1981(PB82 140 385)A03

UCB/EERC-81/07   "The Seismic Resistant Design of Reinforced Concrete Coupled Structural Walls," by A.E. Aktan and V.V.
Bertero - June 1981(PB82 113 358)A11

UCB/EERC-81/08   "The Undrained Shearing Resistance of Cohesive Soils at Large Deformations," by M.R. Pyles and H.B.
Seed - August 1981

UCB/EERC-81/09   "Experimental Behavior of a Spatial Piping System with Steel Energy Absorbers Subjected to a Simulated
Differential Seismic Input," by S.F. Stiemer, W.G. Godden and J.M. Kelly - July 1981

UCB/EERC-81/10 "Evaluation of Seismic Design Provisions for Masonry in the United States," by B.I. Sveinsson, R.L. Mayes and H.D. McNiven - August 1981

UCB/EERC-81/11 "Two-Dimensional Hybrid Modelling of Soil-Structure Interaction," by T.-J. Tzong, S. Gupta and J. Penzien - August 1981(PB82 142 118)A04

UCB/EERC-81/12 "Studies on Effects of Infills in Seismic Resistant R/C Construction," by S. Brokken and V.V. Bertero - September 1981

UCB/EERC-81/13 "Linear Models to Predict the Nonlinear Seismic Behavior of a One-Story Steel Frame," by H. Valdimarsson, A.H. Shah and H.D. McNiven - September 1981(PB82 138 793)A07

UCB/EERC-81/14 "TLUSH: A Computer Program for the Three-Dimensional Dynamic Analysis of Earth Dams," by T. Kagawa, L.H. Mejia, H.B. Seed and J. Lysmer - September 1981(PB82 139 940)A06

UCB/EERC-81/15 "Three Dimensional Dynamic Response Analysis of Earth Dams," by L.H. Mejia and H.B. Seed - September 1981 (PB82 137 274)A12

UCB/EERC-81/16 "Experimental Study of Lead and Elastomeric Dampers for Base Isolation Systems," by J.M. Kelly and S.B. Hodder - October 1981

UCB/EERC-81/17 "The Influence of Base Isolation on the Seismic Response of Light Secondary Equipment," by J.M. Kelly - April 1981

UCB/EERC-81/18 "Studies on Evaluation of Shaking Table Response Analysis Procedures," by J. Marcial Blondet - November 1981

UCB/EERC-81/19 "DELIGHT.STRUCT: A Computer-Aided Design Environment for Structural Engineering," by R.J. Balling, K.S. Pister and E. Polak - December 1981

UCB/EERC-81/20 "Optimal Design of Seismic-Resistant Planar Steel Frames," by R.J. Balling, V. Ciampi, K.S. Pister and E. Polak - December 1981

UCB/EERC-82/01 "Dynamic Behavior of Ground for Seismic Analysis of Lifeline Systems," by T. Sato and A. Der Kiureghian - January 1982 (PB82 218 926) A05

UCB/EERC-82/02 "Shaking Table Tests of a Tubular Steel Frame Model," by Y. Ghanaat and R. W. Clough - January 1982 (PB82 220 161) A07

UCB/EERC-82/03 "Experimental Behavior of a Spatial Piping System with Shock Arrestors and Energy Absorbers under Seismic Excitation," by S. Schneider, H.-M. Lee and G. W. Godden - May 1982

UCB/EERC-82/04 "New Approaches for the Dynamic Analysis of Large Structural Systems," by E. L. Wilson - June 1982

UCB/EERC-82/05 "Model Study of Effects on the Vibration Properties of Steel Offshore Platforms," by F. Shahrivar and J. G. Bouwkamp - June 1982

UCB/EERC-82/06 "States of the Art and Practice in the Optimum Seismic Design and Analytical Response Prediction of R/C Frame-Wall Structures," by A. E. Aktan and V. V. Bertero - July 1982.

UCB/EERC-82/07 "Further Study of the Earthquake Response of a Broad Cylindrical Liquid-Storage Tank Model," by G. C. Manos and R. W. Clough - July 1982

UCB/EERC-82/08 "An Evaluation of the Design and Analytical Seismic Response of a Seven Story Reinforced Concrete Frame - Wall Structure," by A. C. Finley and V. V. Bertero - July 1982

UCB/EERC-82/09 "Fluid-structure Interactions: Added Mass Computations for Incompressible Fluid," by J. S.-H. Kuo - August 1982

UCB/EERC-82/10 "Joint-Opening Nonlinear Mechanism: Interface Smeared Crack Model," by J. S.-H. Kuo - August 1982